

1 **Running title:**

2 Absence of isoprene modifies chloroplastidic membranes in poplar

3

4 **Corresponding author:**

5 Prof. Dr. Jörg-Peter Schnitzler, Research Unit Environmental Simulation, Institute of
6 Biochemical Plant Pathology, Helmholtz Zentrum München, 85764 Neuherberg, Germany

7

8 e-mail jp.schnitzler@helmholtz-muenchen.de

9 Phone +49 89 3187 2413

10 Fax +49 89 3187 4431

11

12

13 **Research areas:**

14 System Biology, Biochemistry and Metabolism.

15

16 **Knocking down of isoprene emission modifies the lipid matrix of thylakoid**
17 **membranes and influences the chloroplast ultrastructure in poplar**

18

19 **Violeta Velikova^{1,3}, Constanze Müller², Andrea Ghirardo³, Theresa Maria Rock²,**
20 **Michaela Aichler⁴, Axel Walch⁴, Philippe Schmitt-Kopplin², and Jörg-Peter**
21 **Schnitzler^{3,*}**

22

23 ¹Institute of Plant Physiology, Bulgarian Academy of Sciences, Sofia 1113, Bulgaria

24 ²Research Unit Analytical BioGeoChemistry, Helmholtz Zentrum München, 85764
25 Neuherberg, Germany

26 ³Research Unit Environmental Simulation, Institute of Biochemical Plant Pathology,
27 Helmholtz Zentrum München, 85764 Neuherberg, Germany

28 ⁴Research Unit Analytical Pathology, Helmholtz Zentrum München, 85764 Neuherberg,
29 Germany

30

31 **Summary**

32 The biological function of isoprene emission in plants is closely associated with the structural
33 organization and functioning of plastidic membranes.

34

35 **ABSTRACT**

36 Isoprene is a small lipophilic molecule with important functions in plant protection against
37 abiotic stresses. Here, we studied the lipid composition of thylakoid membranes and
38 chloroplast ultrastructure in isoprene emitting (IE) and non-isoprene emitting (NE) poplars.
39 We demonstrated that the total amount of mono- (MGDG), di-galactosyldiacylglycerols
40 (DGDG), phospholipids (PL), and fatty acids is reduced in chloroplasts when isoprene
41 biosynthesis is blocked. A significantly lower amount of unsaturated fatty acids, particularly
42 linolenic acid (18:3) in NE chloroplasts was associated with the reduced fluidity of thylakoid
43 membranes, which in turn negatively affects PSII photochemical efficiency (Φ_{PSII}). The low
44 Φ_{PSII} in NE plants was negatively correlated with non-photochemical quenching (NPQ) and
45 the energy-dependent (qE) component of NPQ. Transmission electron microscopy revealed
46 alterations in the chloroplast ultrastructure in NE compared with IE plants. NE chloroplasts
47 were more rounded and contained less grana stacks and longer stroma thylakoids, more
48 plastoglobules, and larger associative zones between chloroplasts and mitochondria. These
49 results strongly support the idea that in isoprene-emitting species, the function of this
50 molecule is closely associated with the structural organization and functioning of plastidic
51 membranes.

52

53

54 **INTRODUCTION**

55 Isoprene is globally the most abundant biogenic hydrocarbon constitutively emitted from
56 many plant species (Guenther et al., 2012). It has been proposed that leaf isoprene emission is
57 an important adaptation for plants, conferring tolerance to different environmental constraints
58 (Vickers et al., 2009; Loreto and Schnitzler, 2010; Loreto and Fineschi, 2014). However,
59 biogenic isoprene emission represents a non-trivial carbon loss in plants, particularly under
60 stress conditions (Fang et al., 1996; Brillì et al., 2007; Teuber et al., 2008; Ghirardo et al.,
61 2014), and the reason(s) why plants emit isoprene are still ambiguous, and the true role of
62 isoprene emission remains elusive. Different approaches and techniques have been used to
63 determine whether and how the cost of this “expensive” carbon emission is matched by the
64 accomplishment of the physiological function *in planta*. It has been shown that isoprene
65 might quench and/or regulate reactive oxygen and nitrogen species formation (Behnke et al.,
66 2010a; Velikova et al., 2012), therefore indirectly providing a general antioxidant action
67 (reviewed in Vickers et al., 2009; Loreto and Schnitzler, 2010) and stabilizing thylakoid

68 membrane structures due the lipophilic properties of this molecule (Sharkey et al., 2001;
69 Velikova et al., 2011).

70 Protein and pigment-protein complexes are assembled and embedded in a lipid matrix,
71 which has a unique lipid composition. The thylakoid lipid bilayer of chloroplasts is
72 characterized as a high proportion of galactolipids with one (monogalactosyldiacylglycerol,
73 MGDG) or two (digalactosyldiacylglycerol, DGDG) galactose molecules (Joyard et al., 2010).
74 MGDGs are the primary constituents (~50%) of thylakoid membrane glycerolipids, followed
75 by DGDGs (~30%), sulfoquinovosyl diacylglycerol (SQDG, ~5-12%) and
76 phosphatidylglycerol (PG, 5-12%) (Kirchhoff et al., 2002). Galactolipids contain a large
77 proportion of polyunsaturated fatty acids, and consequently the thylakoid membrane is a
78 relatively fluid system (Gounaris and Barber, 1983) compared with other biological
79 membranes. The fluidity of the thylakoid membrane is essential for photosynthetic processes.

80 The thylakoid membranes are highly organized internal membrane chloroplast systems that
81 conduct the light reactions of photosynthesis. These membranes comprise pigments and
82 proteins organized in complexes. Thylakoid membranes are arranged into stacked and
83 unstacked regions called grana and stroma thylakoids, respectively, differentially enriched in
84 photosystem I (PSI) and photosystem II (PSII) complexes (Mustárdy et al., 2008). The spatial
85 separation of the PSI and PSII complexes in the stacked and unstacked membrane regions and
86 the macromolecular organization of PSII in stacked grana thylakoids are self-organizing
87 processes and important features to maintain the functional integrity of the photosynthetic
88 apparatus (Kirchhoff et al., 2007).

89 It is not known how changes in the lipid matrix affect lipid-protein interactions and *vice*
90 *versa*, and how membrane macro-organization ensures the efficient diffusion of protein
91 complexes, associated with plant adaptation to the changing environment remains elusive.
92 The isoprene impact on thylakoid intactness and functionality has been assessed using
93 different biophysical techniques (Velikova et al., 2011). Thermoluminescence data
94 demonstrated that the position of the main peak (Q_B peak) was up-shifted approximately 10°C
95 in isoprene emitting plants, suggesting modifications in the lipid environment due to the
96 presence of isoprene in heterologous *Arabidopsis* plants expressing the isoprene synthase
97 gene from poplar. It was also shown that isoprene improves the stability of PSII light-
98 harvesting complexes (LHCII-PSII) through the modification of pigment-protein complex
99 organization in thylakoid membranes (Velikova et al., 2011). Moreover, we recently showed
100 that knocking down isoprene emission in poplar remodels the chloroplast proteome (Velikova
101 et al., 2014). The lack of isoprene resulted in the down-regulation of proteins associated with

102 the light reactions of photosynthesis, redox regulation and oxidative stress defenses and
103 several proteins responsible for lipid metabolism (Velikova et al., 2014).

104 In the present study, we focused on the lipid composition of thylakoid membranes in
105 isoprene-emitting (IE) and non-emitting (NE) poplar leaves. Specifically, we determined
106 whether the translational suppression of isoprene synthase in NE leaves influences the lipid
107 matrix of thylakoids and how this phenomenon affects membrane structure and function. Here
108 we provided evidence that the suppression of isoprene biosynthesis in poplar (i) reduced total
109 galactolipids, phospholipids, and linolenic fatty acid (18:3), (ii) altered the chloroplast
110 ultrastructure, and (iii) stimulated photoprotective mechanisms.

111

112

113 **RESULTS**

114

115 **Lipid, fatty acid and malondialdehyde analyses**

116 Chloroplast membranes isolated from NE poplar had significantly lower (-53%, $P < 0.01$)
117 lipid contents than the membranes of IE plants (Fig. 1). In both NE and IE plants, the major
118 molecular species of MGDG were 18:2-18:3 and 18:3 dimers. In DGDG the major molecular
119 species were n16:0-18:3 and 18:3 dimers. Linolenic acid (18:3) was the major fatty acid of
120 both IE and NE chloroplast membranes, but the content of this fatty acid was consistently
121 much lower in NE than in IE plants (Table 1, Fig. S1). The fatty acid analysis also revealed
122 significantly lower palmitic (n16:0), linoleic (18:2) and stearic (n18:0) acid contents in NE
123 plants compared with IE plants. In the fraction of the phospholipids (PL) the phosphatidic
124 acid (18:1) levels were lower in NE plants.

125 The concentration of malondialdehyde (MDA), the principal product of polyunsaturated
126 fatty acid peroxidation, was lower in chloroplasts isolated from NE plants than in those
127 isolated from IE poplars (Fig. 2), associated with a lower concentration of polyunsaturated
128 fatty acids in NE chloroplasts (Table 1, Fig. S1).

129

130 **Chloroplast ultrastructure observations and protein abundance in photosynthetic** 131 **membranes**

132 To determine whether the different lipid concentrations and changes in lipid composition
133 affect the chloroplast structure, thin leaf segments obtained from the middle region of IE and
134 NE leaves were subjected to Transmission Electron Microscopy (TEM) analyses.

135 Representative micrographs of chloroplasts from IE and NE specimens are shown in Fig. 3
136 and 4.

137 The typical elliptic shape of mesophyll chloroplasts was more oval in NE than in IE
138 specimens (Fig. 3). The mesophyll cells of IE leaves are characterized by a well-developed
139 inner membrane system, comprising grana of different sizes and relatively long stromal
140 thylakoids. IE chloroplasts contained single, midsize starch granules, less numerous
141 peroxisomes, and these organelles were associated with relatively small-sized mitochondria
142 (Fig. 3A, B and 4A, B).

143 Conversely, the chloroplasts of NE plants were characterized by a less developed
144 membrane system, with shorter and fewer grana stacks and longer stroma thylakoids (Fig. 4 C,
145 D, E). NE chloroplasts contained more plastoglobules and smaller starch grains than IE
146 chloroplasts (Fig. 3C, D). NE chloroplasts were also in close structural contact with
147 mitochondria through relatively large associative regions (Fig. 4C). A relatively large number
148 of NE chloroplasts were undeveloped (data not shown).

149 To further understand how the structural changes were related with the protein enrichment
150 in photosynthetic membranes we extracted MS data from our recent proteome study
151 (Velikova et al., 2014). The concentrations of PSI-RCI and PSII-RCII were strongly
152 decreased in NE chloroplasts compare to IE (Fig. 5A, B). Lower protein abundance of PSII-
153 RCII correlated with less number of stacks (Fig. 4F). Chlorophyll concentrations in the NE
154 lines RA1 and RA2 were also significantly reduced (Fig. 5C).

155

156 **Chlorophyll fluorescence**

157 We measured light- and dark-adapted states of chlorophyll fluorescence in IE and NE
158 poplar plants grown under ambient greenhouse conditions (Fig. 6). There was no significant
159 difference in maximal PSII activity between IE and NE plants (data not shown), suggesting
160 that the efficiency of PSII, when all reaction centers were open, was similarly high in both
161 groups of plants. However, NE leaves exhibited significantly lower Φ_{PSII} and qL and higher
162 NPQ (non-photochemical quenching) and qE (energy-dependent quenching) (Fig. 6).
163 Importantly, the true efficiency of PSII (Φ_{PSII}) was lower in NE compared with IE, indicating
164 that a smaller fraction of the absorbed light energy was used for photochemistry. Indeed, the
165 accurate indicator of the PSII redox state, qL, (Baker, 2008), was significantly lower in NE,
166 suggesting that the fraction of open PSII reaction centers was much lower in these mutants
167 (Figs 5, 7, Fig. S2).

168

169 **Multivariate data analyses**

170 We examined the involvement of lipid content and fatty acid compositions in NE and IE
171 chloroplasts, compared with chlorophyll fluorescence measurements, MDA contents and
172 previously described proteomic differences (Velikova et al., 2014). The principal component
173 (PC) analysis showed that the isoprene emission traits reflected the largest variance of the
174 measured data, indicated by the separation between NE and IE samples in the first two
175 principal components (Fig. S2; explained variance: PC1=51%, PC2=16%). Additionally,
176 there were no appreciable differences within the two groups, as both RA1 and RA2 lines and
177 WT and EV lines clustered together in the NE and IE groups, respectively.

178 We performed a discriminant analysis to determine which of the analyzed parameters were
179 significantly affected by the suppression of isoprene biosynthesis and assess the relative
180 importance of these parameters in distinguishing NE from IE plants (Fig. 7). The OPLS
181 analysis indicated, overall, that differences between NE and IE chloroplasts reflect the lipid
182 composition, fatty acid and MDA content, chlorophyll fluorescence parameters and
183 chloroplastic proteins associated with photosynthesis or cell structure. Each singular factor
184 had a different importance (Fig. 7C). Specifically, the most important (high VIP values)
185 variables negatively correlated with NE (positive and high correlation coefficient values)
186 were MDA, qL, PL, saturated and unsaturated fatty acids, the MGDG and DGDG, and
187 photosynthetic proteins (Fig. 7B, C). Importantly, the unsaturated fatty acid 18:3 (linolenic
188 acid) was strongly negatively correlated with NE in all lipids (MGDG, DGDG and PL).
189 Additionally, linolenic acid was well correlated with the lipid degradation product MDA,
190 detected in both MGDG and DGDG. The PL content was highly correlated with
191 photosynthetic proteins, namely PSI proteins, ATP synthase, cytochrome *b₆f* and PsbP.
192 Conversely, NPQ and qE were strongly and positively correlated with the NE genotype.

193 The computed OPLS model was reliable, resulting in a significant ($P = 0.00061$, CV-
194 ANOVA) cross-validated predictive ability of $Q^2(Y) = 84\%$ to distinguish NE from IE
195 samples and a cross-validated goodness of $R^2(X) = 44\%$, $R^2 = 93\%$, $R^2(Y) = 100\%$ using only
196 the first PC.

197

198

199 **DISCUSSION**

200

201 **Suppression of isoprene biosynthesis decreases the chloroplastic lipid content and alters** 202 **chloroplast ultrastructure**

203 One of the proposed biological functions of isoprene is the stabilization of thylakoid
204 membrane structures through the modification of the lipid environment and organization of
205 the pigment-protein complexes in thylakoid membranes (Velikova et al., 2011). Indeed,
206 several clear alterations were evident in thylakoid membrane lipids and fatty acid composition
207 due to the translational suppression of isoprene synthase activity in poplar plants. The most
208 important changes in NE chloroplasts were the absolute decrease in the contents of
209 galactolipids (MGDG, DGDG) and phospholipids (PL) through the down-regulation of the
210 unsaturated fatty linolenic acid (18:3). The functional role of MGDGs in the bioactivity of
211 various membrane proteins is well known (Lee 2003, 2004): a mutant with a defective
212 MGDG synthase 1 (*mgd1*) is unable to produce photosynthetically active membranes
213 (Kobayashi et al., 2013). MGDGs are essential for the efficient activity of violaxanthin de-
214 epoxidase (VDE) (Yamamoto and Higashi, 1978). The ability of the lipid mixture to
215 segregate into bilayer and non-bilayer phases might regulate the protein content in chloroplast
216 membranes (Garab et al., 2000). Indeed, we could demonstrate that the proteins related to
217 photosynthesis were strongly down-regulated in NE compared to IE plants (Fig. 7 and Fig. 8;
218 Velikova et al., 2014).

219 DGDGs are the predominant bilayer lipid species in thylakoid membranes of higher plants
220 (Joyard et al., 2010). They exert structural functions and improve the thermal stability of
221 membranes, particularly at high temperatures (Krumova et al., 2010). DGDGs bind to PSII
222 (Loll et al., 2007) through the formation of hydrogen bonds with tyrosine in PSII (Gabashvili
223 et al., 1998), and DGDGs are also important for binding of extrinsic proteins required for the
224 stabilization of the oxygen-evolving complex (Sakurai et al., 2007). Our data clearly indicate
225 that the suppression of isoprene biosynthesis significantly diminished the level of DGDGs in
226 poplar chloroplasts, which was accompanied with a reduction of the RCI and RCII
227 concentration (Fig. 5A, B), PsbP and PsbQ protein subunits of PSII, and LHCI and LHCII
228 (Velikova et al., 2014). When the thylakoid membrane protein complexes were resolved by
229 blue native-PAGE, the protein patterns of the two groups of poplar lines looked quite similar
230 in content and intensity of the individual bands (Velikova et al., 2014, see supporting
231 information). However, semi-quantitative analysis of the individual protein bands showed that
232 the levels of PSI, the PSII dimer, ATP synthase, the PSII monomer, and the cytochrome *b₆f*
233 complex were slightly reduced in NE compared with IE chloroplasts (Velikova et al., 2014).

234 Decreased lipid and protein levels were associated with changes in the ultrastructure of the
235 chloroplasts from NE plants, suggesting a role for isoprene biosynthesis in the structural
236 organization of plastidic membranes. These results are consistent with previous studies that

237 indicated a role for MGDGs and DGDGs in the structure of thylakoid membranes (Dörmann
238 et al., 1995; Jarvis et al., 2000). In the present study we observed significant reduction of
239 grana stacks per chloroplasts in NE compare to IE poplar lines (Fig. 4E, F), which was related
240 to important decrease in PSI and PSII proteins (Fig. 5A, B). Alterations in protein
241 stoichiometry could exert a direct influence on the thylakoid membrane ultrastructure (Pribil
242 et al., 2014), in particular, the assembly of PSII and LHCII into super- and megacomplexes
243 (Kouřil et al., 2012). It was demonstrated (Labate et al., 2004) that the constitutive expression
244 of the pea *Lhcb 1* gene in transgenic tobacco plants leads to increased grana stacking
245 indicating that increased concentrations of LHCII results in more stacking.

246 Typically, chloroplast membranes have a unique lipid composition characterized by a high
247 proportion of galactolipids containing a large portion of tri-unsaturated fatty acids (C₁₆ or C₁₈)
248 (Joyard et al., 2010). The high content of tri-unsaturated fatty acids guarantees the high
249 fluidity of the thylakoid membranes and the precise allocation of the photosynthetic
250 machinery to efficiently acquire light energy (Gounaris and Barber, 1983). The level of
251 membrane viscosity is an important factor for the photosynthetic performance, e.g., providing
252 the optimal conditions for the diffusion of hydrophobic molecules, such as plastoquinol
253 (Kirchhoff et al., 2000, 2002) or membrane intrinsic protein complexes (e.g., during state
254 transitions) (Allen and Forsberg, 2001; Tikkanen et al., 2008). The low linolenic acid (18:3)
255 content in all lipid fractions from NE chloroplasts indicates that in the absence of isoprene,
256 the thylakoid membrane fluidity is reduced, which in turn negatively affects the efficiency of
257 PSII photochemistry (Fig. 6). A low level of unsaturation in thylakoid membranes makes PSII
258 extremely susceptible to photoinhibition and causes a significant reduction in the content of
259 D1 protein (the reaction center protein) at high irradiance (Kanervo et al., 1995), suggesting
260 that membrane fluidity is a critical factor for PSII D1 protein turnover. Moreover, we detected
261 in NE chloroplast lower amounts of phosphatidic acid (18:1), an important intermediate in
262 lipid biosynthesis (Joyard et al., 2010) with functions as signaling lipid (Testerink and
263 Munnik, 2005, 2011; Horváth et al., 2012; McLoughlin and Testerink, 2013).

264 We observed that the lower level of linolenic acid (18:3) detected in NE chloroplasts was
265 associated with significantly lower MDA chloroplast content in NE compared with IE poplars
266 (Fig. 2, Table 1). Previous studies have reported that MDA is primarily derived from tri-
267 unsaturated fatty acids in chloroplasts (Yamauchi et al., 2008; Schmid-Siegert et al., 2012).
268 MDA can be used as an oxidative stress marker when plants are exposed to unfavorable
269 conditions (Esterbauer et al., 1991), but is also present in healthy plants (Weber et al., 2004;
270 Mène-Saffrané et al., 2007, 2009). On a whole leaf extract level, MDA levels were found

271 higher in NE (Behnke et al., 2010b), which agree with their higher concentrations of linolenic
272 acid (Way et al., 2013). The production of MDA from tri-unsaturated fatty acids serves to
273 adsorb a portion of the reactive oxygen species (ROS) (Mène-Saffrané et al., 2009) and
274 therefore MDA is a by-product in the mechanism of cell protection.

275 Another remarkable observation in the present study was the increased abundance of
276 plastoglobules in NE compared with IE chloroplasts. Plastoglobules are lipoprotein particles
277 containing isoprenoid-driven metabolites (primarily prenylquinones, including plastoquinone
278 and phyloquinone), tocopherols (Vidi et al., 2006) and structural proteins (plastoglobulins)
279 (Bréhélin et al., 2007). The increased number of plastoglobules in NE compared with IE
280 chloroplasts might reflect the higher levels of α -tocopherol in leaves of these lines as
281 previously demonstrated (Behnke et al., 2010b).

282 Electron tomography revealed that plastoglobules are physically coupled to thylakoid
283 membranes via a half-lipid bilayer, providing a direct lipid conduit for metabolite channeling
284 between plastoglobules and thylakoid membranes (Austin et al., 2006). Moreover,
285 plastoglobules are involved in different secondary metabolism pathways, stress responses, and
286 in the development of thylakoids (Bréhélin et al., 2007). In a previous study, we showed that
287 the PAP fibrillin content, comprising lipid-associated proteins (PAPs) and fibrillins, is
288 negatively correlated with the NE plants (Velikova et al., 2014). This observation suggests the
289 involvement of isoprene in the maintenance of thylakoid membranes.

290 Interestingly, we observed larger associative zones between chloroplasts and mitochondria
291 in NE plants. Mitochondria are instrumental for the generation of metabolic energy in
292 eukaryotic cells, and these organelles deliver intermediates to support different metabolic
293 pathways, including photosynthesis (Jacoby et al., 2012). One of the important benefits of
294 mitochondria-chloroplast interactions is the optimization of photosynthetic carbon
295 assimilation through the coordinated production and utilization of ATP and NADPH, the
296 induction of photosynthesis, the activation of enzymes and the maintenance of metabolite
297 levels (Raghavendra and Padmasree, 2003). We propose that the larger associative zones
298 between chloroplasts and mitochondria in NE plants reflect a higher demand for assimilatory
299 power (ATP and NADPH) compared with IE. Indeed, the down-regulation of the cytochrome
300 *b₆f* complex in NE chloroplasts indicates the inhibition of ATP production, associated with
301 the down-regulation of extrinsic subunits of ATP synthase in isoprene-suppressed lines
302 (Velikova et al., 2014). Because isoprene functions as protective molecule against oxidative
303 stress (Loreto and Schnitzler, 2010), the isoprene suppression in NE plants might be balanced

304 by enhancing other compensatory protective mechanisms such as photorespiration and
305 oxidative electron transport, which are both mediated by mitochondria.

306 Recent analyses demonstrated that the suppression of isoprene biosynthesis dramatically
307 reduces carbon fluxes throughout the MEP pathway (Ghirardo et al., 2014), followed by the
308 re-allocation of carbon to other pathways, which in turn induces profound metabolic changes,
309 particularly in lipid biosynthesis (Way et al., 2013; Kaling et al., 2015). Thus, at the cellular
310 level, lipid metabolism is up-regulated in NE leaves, whereas at the subcellular level, as
311 shown herein, low levels of galactolipids and phospholipids comprise the structure of NE
312 chloroplasts. These results suggest that the crucial needs of NE plants to maintain the correct
313 fluidity of thylakoid membranes induces the up-regulation of lipid metabolism, including lipid
314 intermediates, likely compensating for the low levels of galactolipids and phospholipids
315 packed into chloroplast membranes. Thus, isoprene might (i) directly improve the fluidity of
316 thylakoid membranes in synergy with galactolipids or (ii) indirectly affect lipid biosynthesis
317 or trafficking into the chloroplast. Whether, the lack of isoprene function or the alteration of
318 the plastidic isoprenoid pathway itself induces changes in the chloroplastidic lipid levels,
319 thereby affecting membrane fluidity, should be examined in future studies.

320

321 **Functional changes relate to structural alterations in NE chloroplasts**

322 We measured light- and dark-adapted states of chlorophyll fluorescence in IE and NE
323 poplar plants grown under unstressed conditions in order to assess whether the structural
324 changes have functional significance as regards the differences in ability to emit isoprene. Our
325 results showed that Φ_{PSII} was lower in NE plants than in IE plants, consistent with previous
326 observations that the proteins involved in photosynthetic processes are down-regulated in NE,
327 potentially decreasing the efficiency of photochemistry of photosynthesis (Fig. 5; Velikova et
328 al., 2014). The lower Φ_{PSII} values in NE were negatively correlated to NPQ, a protective
329 mechanism for the removal of excess excitation energy within pigment complexes and the
330 inhibition of the formation of free radicals (Demmig-Adams and Adams, 2006).

331 Higher NPQ levels in concert with restricted ETR between both photosystems and a
332 reduced plastoquinone pool has been shown (Härtel et al., 1998) to be accompanied by
333 DGDG modifications in the *Arabidopsis* mutant (*dgd1*). Moreover, in this mutant PSI showed
334 an increased capacity for cyclic electron transfer and a reduced capacity for state transitions
335 (Ivanov et al., 2006). Similar to the *dgd1* mutant (Dörmann et al., 1995), the NE poplar plants
336 showed a lower DGDG content, modified chloroplastic ultrastructure, increased NPQ,

337 restricted ETR (Behnke et al., 2007), and decreased total chlorophyll content (Fig. 5C)
338 (Behnke et al., 2013; Way et al., 2013; Ghirardo et al., 2014).

339 The NPQ comprises energy-dependent (i.e., dependent on the energization of thylakoid
340 membranes) quenching (qE), state transitions (qT) (Minagava, 2011), photoinhibition
341 quenching (qI) (Müller et al., 2001), and zeaxanthin-dependent quenching (qZ) (Nilkens et al.,
342 2010). Energy-dependent quenching is the most important and well-characterized component
343 of NPQ. This transition is triggered through the acidification of the thylakoid lumen (Ruban et
344 al., 2012), which in turn leads to the protonation of VDE, for the conversion of violaxanthin
345 to zeaxanthin, and PsbS, a polypeptide of the PSII-associated LHC (Kiss et al., 2008; Murchie
346 and Niyogi, 2011).

347 Here we showed higher values of qE in NE plants, which might reflect a particular
348 conformation of the LHCII complex resulting from chlorophyll and/or xanthophyll/protein
349 interactions (Horton et al., 2005). Indeed, we observed that many proteins associated with
350 photosynthesis are less abundant in NE chloroplasts (Fig. 5 and Fig. 7; for detail see Velikova
351 et al., 2014). This lack of photosynthetic proteins could lead to specific conformational
352 changes, which in turn could determine the higher qE in NE poplars. However, the
353 supramolecular organization of the PSII antenna involves numerous interactions between
354 proteins, suggesting that the changes in these interactions (Garab and Mustardy, 1999; Horton
355 et al., 2005) could be responsible for the increase in NPQ we observed in NE plants. Indeed,
356 with CD spectroscopy it has been shown that isoprene deficiency inhibits the formation of the
357 chirally organized macrodomains. This effect in turn decreases the thermal stability of
358 thylakoid membranes (Velikova et al., 2011). We also observed the significant down-
359 regulation of the cytochrome *b₆f* complex in NE lines (Velikova et al., 2014), which might
360 inhibit the production of ATP in isoprene-suppressed plants. The increase of qE in NE lines
361 might reflect the optimization of electron transport and ATP synthesis through the modulation
362 of the cyclic electron transfer around PSI, the activation state of ATP synthase, and the
363 partitioning of the proton motive force between ΔpH and the membrane electrical potential
364 (Horton et al., 2005).

365

366 CONCLUSION

367 The proposed biological functions of isoprene in plants have been associated with the
368 ability of this molecule to affect thylakoid membrane organization and reduce the formation
369 of ROS, conferring tolerance to heat and oxidative stress. It has been hypothesized that
370 isoprene improves the thermal stability of thylakoid membranes by affecting the membrane

371 lipid composition (Velikova et al., 2011). Herein, we provided direct evidence of the
372 relationship between isoprene emission and the level of main lipid classes and their fatty acid
373 composition, and we characterized the structural organization of the photosynthetic
374 machinery in IE and NE poplar genotypes. The suppressed isoprene production in NE plastids
375 was associated with the reduced amount of galacto- and phospholipids, lower level of the
376 major fatty acid (18:3), and altered chloroplast ultrastructure (Fig. 8). The suppression of
377 isoprene biosynthesis causes considerable metabolic changes, particularly in lipid
378 biosynthesis (Way et al., 2013; Kaling et al., 2015) and significant alterations in the
379 chloroplast proteome (Velikova et al., 2014). The majority of the plastidic and mitochondria
380 proteome is encoded in the nuclear genome, and there is a continuous exchange of “forward”
381 information from nucleus-to-organelle (anterograde) and of “backward” information from
382 organelle-to-nucleus (retrograde) (Pfannschmidt, 2010). According to the retrograde signaling
383 concept, based on the available experimental data, signals originating in chloroplasts and/or
384 mitochondria modulate nuclear gene expression (Leister, 2012). These signals originate from
385 carotenoid biosynthesis, ROS, photosynthetic redox processes, and changes in the pool of
386 metabolites (Pfannschmidt, 2010; Leister, 2012). The plastidic signals identified so far have
387 been associated with specific stress conditions. It is likely that the comprehensive changes in
388 the metabolome (e.g., Way et al., 2013; Kaling et al., 2015), liposome, proteome (Velikova et
389 al., 2014) and ultrastructure of the chloroplasts in non-isoprene emitting poplars (Fig. 8) as
390 well as the distinct physiological behavior of these plants reflects finely tuned retrograde
391 signaling. The precise mechanism(s) for the transmission of the changes in chloroplast to the
392 nucleus in NE plant cells remain elusive.

393

394 **MATERIAL AND METHODS**

395 **Plant material**

396 In the present study, we used the same gray poplar (*Populus x canescens*; syn. *Populus*
397 *tremula x P. alba*) genotypes as utilized in previous chloroplast proteome research (Velikova
398 et al., 2014), namely two isoprene-emitting lines (IE: wild type and empty vector control,
399 WT/EV) and two non-isoprene emitting (NE: RA1/RA2) lines. EV was used to ensure that
400 the differences between NE and IE reflected specific alterations in the isoprene synthase gene
401 and not to a more general genetic manipulation effect. The plants were grown in a greenhouse
402 as previously described (Velikova et al., 2014). Briefly, the ambient temperature was 25/20°C,
403 with a relative humidity of 50/60% and a photoperiod of 16/8 h (day/night). The plants were
404 fertilized weekly with Triabon (Compo, Münster, Germany) and Osmocote (Scotts Miracle-
405 Gro, Marysville, OH) (1:1 v/v; 10 g per liter of soil).

406 Four-month-old plants were used for the experiments. Fully expanded leaves (9th node
407 from the apical meristem) from 6-7 different plants, considered as biological replicates, were
408 used for physiological, biochemical and structural studies. The chloroplasts were isolated as
409 previously described (Velikova et al., 2014) and used for lipid and malondialdehyde (MDA)
410 analyses.

411

412 **Lipid extraction procedure**

413 The total lipids from chloroplasts were extracted according to Bligh and Dyer (1959). All
414 procedures were performed in dim light using chilled solvents (containing BHT, 0.01% w/v)
415 and glassware. The chloroplast samples (0.5 mL) were mixed with chloroform/methanol (1:2
416 v/v; 1.9 mL) for approximately 2 min, and subsequently 0.625 mL of chloroform and 0.625
417 mL of distilled water were added. The lower chloroform phase, containing the lipids, was
418 removed, and aliquots were transferred into vials and exsiccated under N₂. The residues were
419 weighed and calculated for total lipids.

420

421 **GC-MS analysis of phospholipid fatty acid composition**

422 Phospholipid fatty acids (PLFAs) were analyzed as previously described (Way et al., 2013;
423 Behnke et al., 2013). Briefly, the PLFAs were separated from other lipids using a silica
424 bonded phase column (MEGA-BE-SI, 2 g 12 mL⁻¹, 20/PK, Bond ELUT, Agilent
425 Technologies, CA, USA). Fatty acid methyl esters (FAMES) were obtained after mild alkaline
426 hydrolysis. Myristic acid was used as internal standard for gas chromatography analysis. Un-
427 substitute FAMES were measured using a 5973MSD GC-MS (Agilent Technologies,
428 Oberhaching, Germany) coupled with a combustion unit to an isotope ratio mass spectrometer
429 (DeltaPlus; Thermo Electron Corporation, Bremen, Germany) and identified using the
430 established fatty acid libraries and characteristic retention times of pure standards. The fatty
431 acids were named according to the total number of C atoms and double bonds. Saturated
432 straight-chain fatty acids are indicated as 'n'.

433

434 **UPLC-ESI-Qq-ToF-MS of galactolipids**

435

436 Lipids were dissolved in 1 mL of LC-MS grade methanol (Fluka). MGDG and DGDG
437 contents were analyzed using the UPLC-ESI Qq-ToF-MS System (Ultra performance liquid
438 chromatography electrospray time of flight mass spectrometry, maXis Bruker, Bremen,
439 Germany). Aliquots of 2.5 µL of each sample were analyzed in three technical replicates in
440 randomized order.

441 The chromatographic separation was achieved on a C₁₈ ACQUITYUPLC BEH column, 50
442 mm, 2.1 mm, and 1.7 μm (Waters), using a gradient elution. The composition was changed
443 from 50% to 92% B for 10 min and maintained for an additional 10 min, then change to 100%
444 B for 1 min and maintained for 5 min. The flow was set to 0.4 mL h⁻¹. Mobile phase A
445 comprised water/isopropyl alcohol (95:5, v/v), and mobile phase B comprised
446 acetonitrile/isopropyl alcohol (95:5, v/v). A format of 0.001 mM sodium (Sigma-Aldrich,
447 Taufkirchen, Germany) was added to both mobile phases. This method has been previously
448 published for profiling photosynthetic glycerol lipids (Xu et al., 2010).

449 MGDGs and DGDGs were detected as sodium adducts through positive electrospray
450 ionization. The instrument was calibrated with ESI tune mix (Agilent Technologies).
451 Acquired spectra were internally calibrated and exported to GENEDATA software for
452 chromatographic alignment and peak picking. MGDGs and DGDGs were identified based on
453 the retention time and detected exact mass (mass error < 0.01 Da).

454 MGDG and DGDG standards (Larodan) were used to evaluate the analytical performance
455 and determine the QC, which was injected 10 times in the beginning for column conditioning
456 and after every 10th sample to validate the measuring performance.

457

458 **Malondialdehyde (MDA) content**

459 The lipid peroxidation level in extracted chloroplast samples was quantified after
460 measuring the MDA content using the thiobarbituric acid-reactive substances (TBARS) assay
461 according to Hodges et al. (1999). The chloroplast sample (0.100 mL) was mixed with 1.2 mL
462 of 80% ethanol (containing 0.01% BNT w/v) and sonicated in a water bath sonicator for 3
463 min, followed by centrifugation at 5,000 g for 10 min at 4°C. An aliquot of the obtained
464 supernatant (0.5 mL) was mixed with the same volume of 0.65% (w/v) thiobarbituric acid
465 (TBA) solution containing 20% (w/v) trichloroacetic acid (TCA). Another aliquot of the
466 supernatant (0.5 mL) was mixed with 0.5 mL of 20% (w/v) TCA, representing the zero-
467 control. The mixture was heated at 95°C for 30 min. The reaction was terminated after
468 incubation in an ice bath. The cooled mixture was centrifuged at 10,000 g for 10 min at 4°C,
469 and the absorbance of the supernatant was measured at 532, 600 and 440 nm (Perkin Elmer,
470 Walthman, MSC, USA). MDA equivalents were calculated according to Hodges et al. (1999),
471 namely:

472 1) $[A_{532+TBA} - A_{600+TBA} - (A_{532-TBA} - A_{600+TBA})] = A$

473 2) $[(A_{440+TBA} - A_{600+TBA}) \times 0.0571] = B$

474 3) MDA equivalents (nmol mL⁻¹) = $(A - B)/157000 \times 10^6$

475

476 **Protein and chlorophyll analysis**

477 For the calculation of the abundance of reaction center proteins in PSI and PSII we used
478 the chloroplast proteome data published in Velikova et al. (2014). Peak intensities of peptides
479 identified as RCI (protein accession numbers: POPTR_0008s15100.1, POPTR_0006s27030.1,
480 POPTR_0003s14870.1, POPTR_0002s25510.2) and RCII (protein accession numbers:
481 POPTR_0011s03390.1, POPTR_0004s03160.1, POPTR_0005s22780.1, POPTR_0002s05660.1,
482 POPTR_0005s01430.1, POPTR_0005s27800.3, POPTR_0002s05720.1, POPTR_0002s25810.1,
483 POPTR_0001s44210.1, POPTR_0006s26270.1), respectively, were summed, and expressed per
484 mg chlorophyll.

485 The chlorophyll content was measured in isolated chloroplast suspension after extraction
486 with 80% of ice-cold acetone. Absorbance at 663 and 646 nm was detected to determine
487 chlorophyll a and chlorophyll b concentrations, calculated according to Porra et al. (1989).

488

489 **Chlorophyll fluorescence measurements**

490 The chlorophyll fluorescence parameters were measured on intact leaves using a MINI-
491 PAM Photosynthesis Yield Analyzer (Heinz Walz GmbH, Effeltrich, Germany). The leaves
492 were dark-adapted for 15 min prior to the determination of the minimal (F_o) and maximal (F_m)
493 chlorophyll fluorescence, and subsequently the leaves were exposed to actinic light ($430 \mu\text{mol}$
494 $\text{m}^{-2} \text{s}^{-1}$). After steady-state fluorescence was obtained, a saturating pulse was applied to
495 determine the maximum fluorescence in the light (F_m'). The operating efficiency of PSII
496 photochemistry (Φ_{PSII}) was calculated from $(F_m' - F')/F_m'$ (Genty et al., 1989). The redox
497 state of PSII was assessed based on the parameter $qL = (F_q'/F_v')/(F_o'/F')$, where F' is the
498 fluorescence emission from the light-adapted leaf, F_v' - variable fluorescence from the light-
499 adapted leaf, and F_q' is the difference in fluorescence between F_m' and F' (Baker, 2008); F_o'
500 was estimated using the following equation: $F_o' = F_o/[(F_v/F_m) + F_o/F_m']$ (Oxborough and
501 Baker, 1997). The non-photochemical quenching (NPQ) was calculated as $\text{NPQ} = (F_m -$
502 $F_m')/F_m'$ (Bilger and Björkman, 1991). The NPQ relaxation kinetics in the dark was used to
503 calculate energy-dependent (qE) quenching. qE was assigned as a fast-relaxing component
504 (within the first 2 minutes of dark relaxation after switching off the actinic light), calculated
505 as $qE = (F_m'' - F_m')/F_{m, 2\text{min dark}}''$ (Zaks et al., 2013).

506

507 **Transmission Electron Microscopy (TEM)**

508 Leaf segments (1 mm²) were cut from the middle of the leaves for TEM analyses. The
509 segments were fixed in 2.5% (v/v) glutaraldehyde (electron microscopy grade) in 0.1 M
510 sodium cacodylate buffer, pH 7.4 (Science Services, Munich, Germany), post-fixed in 2%
511 (v/v) aqueous osmium tetroxide (Dalton, 1955), dehydrated in gradual ethanol (30–70%),
512 stained with uranyl acetate (2% in 70% ethanol), dehydrated in gradual ethanol (70-100%)
513 and propylene oxide (100%), embedded in Epon (Merck, Darmstadt, Germany) and cured for
514 24 h at 60°C. Semi-thin sections (300 nm) were cut and stained with toluidine blue. Ultrathin
515 sections of 50 nm were collected onto 200 mesh copper grids before examination using
516 transmission electron microscopy (Zeiss Libra 120 Plus, Carl Zeiss NTS GmbH, Oberkochen,
517 Germany). The images were acquired using ‘Slow Scan CCD-camera’ and ‘iTEM’ software
518 (Olympus Soft Imaging Solutions, Münster, Germany).

519

520 **Statistical analyses**

521 Correlation analyses between different data sets of phospholipid (PL) and galactolipid
522 (MGDG, DGDG) contents, fatty acid compositions, chlorophyll fluorescence parameters,
523 MDA content, the data groups and IE or NE genotypes were performed using Principal
524 Component Analysis (PCA) and Orthogonal Partial Least Square regression (OPLS) from the
525 software package ‘SIMCA-P’ (v13.0.0.0, Umetrics, Umeå, Sweden). In addition, we included
526 the chloroplastic protein contents associated with photosynthesis and structure (Velikova et al.,
527 2014) to correlate lipids to proteins. Because the proteomic data originated from 3 samples for
528 each plant genotype (containing 6 - 7 different leaves each of the three samples), multivariate
529 analyses were performed using only the data matching the same 3 samples used for both
530 proteomic and PL analyses. Galactolipids, MDA, and chlorophyll fluorescence measurements
531 were obtained from more and different extracts, and therefore only the data from 3 samples
532 were taken randomly and used for these analyses. We added the means of all biological
533 replicates to examine the correlations between genotypes using data originating from different
534 leaf extracts. The resulting matrix size was therefore 78-by-16 (variables-by-observations).
535 Thus, the present analyses could correlate any data value with an isoprene emission trait
536 (plant genotype IE and NE), but correlations between/within variables could be achieved only
537 using data from the same leaf material, i.e., within PL and proteins, MGDG, DGDG and
538 MDA, and within chlorophyll fluorescence data.

539 The multivariate data analyses followed the established procedures to analyze MS data as
540 previously described (Ghirardo et al., 2005; Ghirardo et al., 2012; Kreuzwieser et al., 2014;
541 Vanzo et al., 2014; Velikova et al., 2014). The isoprene emission trait was selected as the Y-

542 variable for the OPLS analysis by setting NE = 1 and IE = 0. The X variables were centered,
543 and each type of data was block-wise scaled with 1 sd^{-1} , considering the different number of
544 X-variables in each group of data. Each calculated significant principal component was
545 validated using ‘full cross validation’, with 95% confidence level on parameters. The
546 regression model OPLS was further tested for significance using CV-ANOVA (Eriksson et al.,
547 2008). Variables showing variable of importance for the projection (VIP) values greater than
548 1 and jack-knifing method uncertainty bars smaller than the respective VIP values were
549 defined as discriminant variables to distinguish IE from NE samples. For the proteomics data,
550 containing a much higher number of variables, the VIP threshold was set to 0.5. The statistical
551 significance of the differences between the means of discriminant variables and the functional
552 and structural parameters measured in NE and IE plants were additionally evaluated using
553 Student’s *t*-test and at an α level of 0.05, unless otherwise stated.

554

555 **Legend to figures:**

556

557

558 **Figure 1.** Lipid content in isolated chloroplasts of isoprene emitting (IE, WT/EV) and non-
559 isoprene emitting (NE, RA1/RA2) poplar. Error bars display the SE (n=4). Asterisks indicate
560 significant differences with WT; ** $P < 0.01$.

561

562 **Figure 2.** MDA level in isolated chloroplasts of isoprene emitting (IE, WT/EV) and non-
563 isoprene emitting (NE, RA1/RA2) poplar. Error bars display the SE (n=4). Asterisks indicate
564 significant differences with WT; * $P < 0.05$.

565

566 **Figure 3.** Transmission electron micrographs of representative chloroplast cross-sections
567 taken from the intact leaves of isoprene emitting (IE, WT/EV) (A, B) and non-isoprene
568 emitting (NE, RA1/RA2) (C, D) poplar. Height / Length ratio (E) and average number of
569 starch grains in IE and NE chloroplasts (F). CW - cell wall; GT - granal thylakoids; M,
570 mitochondrion; P, plastoglobuli; S, stroma; SI, starch gain. Scale bar = 1 μm in A, B, C and D;
571 at x 6,300 magnification.

572

573 **Figure 4.** Transmission electron micrographs of representative chloroplast cross-sections
574 taken from the intact leaves of isoprene emitting (IE, WT/EV) (A, B) and non-isoprene
575 emitting (NE, RA1/RA2) (C, D) poplar. Average number of stacks per chloroplast (E) and
576 correlation between PSII – RCII protein abundance (10 peptides; for protein accession

577 numbers see Materials and Methods) and number of stacks (F). CW - cell wall; GT - granal
578 thylakoids; M, mitochondrion; P, plastoglobuli; S, stroma; SI, starch grain. Scale bar = 500 nm
579 in A, and C, at x10,000 magnification; and 200 nm in B and D, at magnification x20,000.

580

581 **Figure 5.** Protein abundance of PSI-RCI (4 peptides; for protein accession numbers see
582 Materials and methods) (A), PSII-RC (10 peptides; for protein accession numbers see
583 Materials and methods) (B) and chlorophyll content (C) in isoprene emitting (IE, WT/EV)
584 and non-isoprene emitting (NE, RA1/RA2) poplar plants. Protein abundance represents sum
585 of MS data extracted from our proteome study (Velikova et al., 2014). Error bars display the
586 SE (n=4). Asterisks indicate significant differences with WT; ** $P < 0.01$; *** $P < 0.001$.

587

588 **Figure 6.** PSII photochemical efficiency (A), redox state of PSII (B), non-photochemical
589 quenching (C) and NPQ energy-dependent component (D) of isoprene emitting (IE, WT/EV)
590 and non-isoprene emitting (NE, RA1/RA2) poplar plants at growth conditions. Values
591 represent means of 5-7 different plants out of three independent experiments (n = 15–21, \pm SE
592 is given). Photosynthetic parameters are described in “Material and Methods”. Asterisks
593 indicate significant differences with WT; * $P < 0.05$, ** $P < 0.01$, *** $P < 0.001$.

594

595 **Figure 7.** Score (A), loading (B) and correlation coefficient plots (C) of Orthogonal Partial
596 Least Squares (OPLS) of lipid classes, fatty acid composition and MDA contents in isolated
597 chloroplasts, chlorophyll fluorescence parameters measured in intact leaves (NPQ, Φ_{PSII} , qE
598 and qL), and chloroplast proteins related to photosynthesis and proteins with structural
599 activity. (A) IE (WT/EV), grey circles; NE (RA1/RA2), white triangles. (B) Each parameter
600 is indicated with different symbol. Dark grey circles, MGDG; dark gray square, DGDG; gray
601 triangle, PL; dark gray circles with a dot, MGDG – fatty acids; dark gray square with a dot –
602 DGDG – fatty acids; gray triangle with a dot, PL – fatty acids; green diamond, MDA; red star,
603 NPQ; red triangle-down, qE; blue square, qL; blue star, proteins with structural activity; green
604 star, proteins related to photosynthesis. (C) Parameter colors as plot legend B. Only
605 discriminant data with VIP > 1 (for all except proteins) and VIP > 0.5 (proteins) are presented.
606 Model fitness: $Q^2(Y) = 84\%$; $R^2(X) = 44\%$, $R^2 = 93\%$, $R^2(Y) = 100\%$ using one PC; P =
607 0.00061, CV-ANOVA.

608

609 **Figure 8.** Schematic overview of the changes in chloroplast ultrastructure, lipid composition,
610 change, protein abundance and PSII fluorescence triggered by the suppression of isoprene
611 biosynthesis and emission in poplar plants.

612

613

614

615 **Acknowledgements**

616

617 This research was supported by a grand awarded by the Alexander von Humboldt Foundation
618 to V.V.

619

620

621 **Supporting information**

622 Supplemental Figure S1 provides lipid content and fatty acid composition in isolated
623 chloroplasts of isoprene emitting (IE, WT/EV) and non-emitting (NE, RA1/RA2) poplar.

624 Supplemental Figure S2 provides score and loading plots of PCA all parameters analyzed
625 (lipid and fatty acid composition, MDA, NPQ, Φ_{PSII} , qE, qL, proteins related to
626 photosynthesis and proteins with structural activity.

627

628

629 **LITERATURE CITED**

630

631 **Allen JF, Forsberg J** (2001) Molecular recognition in thylakoid structure and function.

632 Trends Plant Sci **6**: 317-326

633 **Austin JR, Frost E, Vidi P-A, Kessler F, Staehelin LA** (2006) Plastoglobules are

634 lipoprotein subcompartments of the chloroplast that are permanently coupled to thylakoid
635 membranes and contain biosynthetic enzymes. Plant Cell **18**: 1693–1703

636 **Baker NR** (2008) Chlorophyll fluorescence: a probe of photosynthesis in vivo. Ann Rev

637 Plant Biol **59**: 89–113

638 **Behnke K, Ehlting B, Teuber M, Bauerfeind M, Louis S, Hänsch R, Polle A, Bohlmann**

639 **J, Schnitzler JP** (2007) Transgenic, non-isoprene-emitting poplars don't like it hot. Plant
640 J **51**: 485-499

641 **Behnke K, Ghirardo A, Janz D, Kanawati B, Esperschütz J, Zimmer I, Schmitt-**

642 **Kopplin P, Niinemets Ü, Polle A, Schnitzler JP, Rosenkranz M** (2013) Isoprene
643 function in two contrasting poplars under salt and sunflecks. Tree Physiol **33**: 562-578

644 **Behnke K, Kaiser A, Zimmer I, Brüggemann N, Janz D, Polle A, Hampp R, Hänsch R,**

645 **Popko J, Schmitt-Kopplin P, Ehlting B, Rennenberg H, Barta C, Loreto F, Schnitzler**

- 646 **JP** (2010a) RNAi-mediated suppression of isoprene emission in poplar impacts phenolic
647 metabolism: a transcriptomic and metabolomic analysis. *Plant Mol Biol* **74**: 61-75
- 648 **Behnke K, Kleist E, Uerlings R, Wildt J, Rennenberg H, Schnitzler JP** (2009) RNAi-
649 mediated suppression of isoprene biosynthesis in hybrid poplar impacts ozone tolerance.
650 *Tree Physiol* **29**: 725-736
- 651 **Behnke K, Loivamäki M, Zimmer I, Rennenberg H, Schnitzler JP, Louis S** (2010b)
652 Isoprene emission protects photosynthesis in sunfleck exposed grey poplar. *Photosyn Res*
653 **104**: 5-17
- 654 **Bilger W, Björkman O** (1991) Temperature dependence of violaxanthin de-epoxidation and
655 non- photochemical fluorescence quenching in intact leaves of *Gossypium hirsutum* L.
656 and *Malva parviflora* L. *Planta* **184**: 226–234
- 657 **Bligh EG, Dyer WJ** (1959) A rapid method for total lipid extraction and purification. *Can J*
658 *Biochem Physiol* **37**: 911-917
- 659 **Bréhélin C, Kessler F, Wijk KJ** (2007) Plastoglobules: versatile lipoprotein particles in
660 plastids. *Trends Plant Sci* **12**: 260-266
- 661 **Brilli F, Barta C, Fortunati A, Lerdau M, Loreto F, Centritto M** (2007) Response of
662 isoprene emission and carbon metabolism to drought in white poplar (*Populus alba*)
663 saplings. *New Phytol* **175**: 244-254
- 664 **Dalton AJ** (1955) A chrome-osmium fixative for electron microscopy. *Anat Record* **121**:
665 281
- 666 **Demmig-Adams B, Adams I WW** (2006) Photoprotection in an ecological context: the
667 remarkable complexity of thermal energy dissipation. *New Phytol* **172**: 11–21
- 668 **Dörmann P, Hoffmann-Benning S, Balbo I, Benning C** (1995) Isolation and
669 characterization of an Arabidopsis mutant deficient in the thylakoid lipid digalactosyl
670 diacylglycerol. *Plant Cell* **7**: 1801–1810
- 671 **Eriksson L, Trygg J, Wold S** (2008) CV-ANOVA for significance testing of PLS and OPLS
672 models. *J Chemom* **22**: 594–600
- 673 **Esterbauer H, Schaur RJ, Zollner H** (1991) Chemistry and biochemistry of 4-
674 hydroxynonenal, malondialdehyde and related aldehydes. *Free Radic Biol Med* **11**: 81-
675 128
- 676 **Fang C, Monson RK, Cowling EB** (1996) Isoprene emission, photosynthesis, and growth in
677 sweetgum (*Liquidambar styraciflua*) seedlings exposed to short- and long-term drying
678 cycles. *Tree Physiol* **16**: 441-446

- 679 **Gabashvili IS, Menikh A, Segui J, Fragata M** (1998) Protein structure of photosystem II
680 studied by FTIR spectroscopy. Effect of digalactosyldiacylglycerol on the tyrosine side
681 chain residues. *J Mol Str* **444**: 123-133
- 682 **Garab G, Lohner K, Laggner P, Farkas T** (2000) Self-regulation of the lipid content of
683 membranes by non-bilayer lipids: a hypothesis. *Trends Plant Sci* **5**: 489-494
- 684 **Garab G, Mustardy L** (1999) Role of LHCII-containing macrodomains in the structure,
685 function and dynamics of grana. *Aust J Plant Physiol* **26**: 649–658
- 686 **Genty B, Briantais JM, Baker NR** (1989) The relationship between the quantum yield of
687 photosynthetic electron-transport and quenching of chlorophyll fluorescence. *Biochim*
688 *Bioph Acta* **990**: 87–92
- 689 **Genty B, Goulas Y, Dimon B, Peltier G, Briantais JM, Moya I** (1992) Modulation of
690 efficiency of primary conversion in leaves, mechanisms involved at PS2. In: Murata N, ed.
691 Research in photosynthesis, Vol. IV: Proceedings of IXth International Congress on
692 Photosynthesis. Nagoya, Japan, August 30–September 4, 603–610,
- 693 **Ghirardo A, Heller W, Fladung M, Schnitzler JP, Schroeder H** (2012) Function of
694 defensive volatiles in pedunculate oak (*Quercus robur*) is tricked by the moth *Tortrix*
695 *viridana*. *Plant Cell Environ* **35**: 2192-2207
- 696 **Ghirardo A, Sørensen HA, Petersen M, Jacobsen S, Søndergaard I** (2005) Early
697 prediction of wheat quality: analysis during grain development using mass spectrometry
698 and multivariate data analysis. *Rapid Commun Mass Spectrom* **19**: 525–532
- 699 **Ghirardo A, Wright LP, Bi Z, Rosenkranz M, Pulido P, Rodríguez-Concepción M,**
700 **Niinemets Ü, Brüggemann N, Gershenzon J, Schnitzler JP** (2014) Metabolic flux
701 analysis of plastidic isoprenoid biosynthesis in poplar leaves emitting and nonemitting
702 isoprene. *Plant Physiol* **165**: 37-51
- 703 **Gounaris K, Barber J** (1983) Monogalactosyldiacylglycerol: the most abundant polar lipid
704 in Nature, *Trends Biochem Sci* **8**: 378–381
- 705 **Guenther AB, Jiang X, Heald CL, Sakulyanontvittaya T, Duhl T, Emmons LK, Wang**
706 **X** (2012) The Model of Emissions of Gases and Aerosols from Nature version 2.1
707 (MEGAN2.1): an extended and updated framework for modeling biogenic emissions.
708 *Geoscientific Model Development* **5**: 1471–1492
- 709 **Härtel H, Lokstein H, Dörmann P, Trethewey RN, Benning C** (1998) Photosynthetic
710 light utilization and xanthophyll cycle activity in the galactolipid deficient *dgd1* mutant of
711 *Arabidopsis thaliana*. *Plant Physiol Biochem* **36**: 407-417

- 712 **Hodges DM, DeLong JM, Forney CF, Prange RK** (1999) Improving the thiobarbituric
713 acid-reactive-substances assay for estimating lipid peroxidation in plant tissues containing
714 anthocyanin and other interfering compounds. *Planta* **207**: 604-611
- 715 **Horton P, Wentworth M, Ruban A** (2005) Control of the light harvesting function of
716 chloroplast membranes: the LHCII-aggregation model for non-photochemical quenching.
717 *FEBS Lett* **579**: 4201-4206
- 718 **Horváth I, Glatz A, Nakamoto H, Mishkind ML, Munnik T, Saidi Y, Goloubinoff P,**
719 **Harwood JL, Vigh L** (2012) Heat shock response in photosynthetic organisms:
720 Membrane and lipid connections. *Progress Lipid Res* **51**: 208-220
- 721 **Ivanov AG, Hendrickson L, Krol M, Selstam E, Öquist G, Hurry V, Huner NPA** (2006)
722 Digalactosyl-diacylglycerol deficiency impairs the capacity for photosynthetic
723 intersystem electron transport and state transitions in *Arabidopsis thaliana* due to
724 photosystem I acceptor-side limitations, *Plant Cell Physiol* **47**: 1146-1157
- 725 **Jacoby RP, Li L, Huang S, Lee CP, Millar AH, Taylor NL** (2012) Mitochondrial
726 composition, function and stress response in plants. *J Integr Plant Biol* **54**: 887-906
- 727 **Jarvis P, Dörmann P, Peto CA, Lutes J, Benning C, Chory J** (2000) Galactolipid
728 deficiency and abnormal chloroplast development in the *Arabidopsis* MGD synthase 1
729 mutant. *Proc Natl Acad Sci USA* **97**: 8175–8179
- 730 **Joyard J, Ferro M, Masselon C, Seigneurin-Berny D, Salvi D, Garin J, Rolland N** (2010)
731 Chloroplast proteomics highlights the subcellular compartmentation of lipid metabolism.
732 *Progress in Lipid Research* **49**: 128-158
- 733 **Kaling M, Kanawati B, Ghirardo A, Albert A, Winkler JB, Heller W, Barta C, Loreto**
734 **F, Schmitt-Kopplin P, Schnitzler JP** (2015) UV-SI: UV-B mediated metabolic
735 rearrangements in poplar revealed by non-targeted metabolomics. *Plant Cell Environ* **38**:
736 892-904
- 737 **Kanervo E, Aro E-M, Murata N** (1995) Low unsaturation level of thylakoid membrane
738 lipids limits turnover of the D1 protein of photosystem II at high irradiance. *FEBS Lett*
739 **364**: 239-242
- 740 **Kirchhoff H, Haase W, Haferkamp S, Schott T, Borinski M, Kubitscheck U, Rögner M**
741 (2007) Structural and functional self-organization of photosystem II in grana thylakoids.
742 *Biochim Biophys Acta* **1767**: 1180 -1188
- 743 **Kirchhoff H, Horstmann S, Weis E** (2000) Control of the photosynthetic electron transport
744 by PQ diffusion microdomains in thylakoids of higher plants, *Biochim Biophys Acta*
745 **1459**: 148-168

- 746 **Kirchhoff H, Mukherjee U, Galla H-J** (2002) Molecular architecture of the thylakoid
747 membrane: Lipid diffusion space for plastoquinone. *Biochem* **41**: 4872-4882
- 748 **Kiss AZ, Ruban AV, Horton P** (2008) The PsbS protein controls the organization of the
749 photosystem II antenna in higher plant thylakoid membranes. *J Biol Chem* **283**: 3972–
750 3978
- 751 **Kobayashi K, Narise T, Sonoike K, Hashimoto H, Sato N, Kondo M, Nishimura M,**
752 **Sato M, Toyooka K, Sugimoto K, Wada H, Masuda T, Ohta H** (2013) Role of
753 galactolipid biosynthesis in coordinated development of photosynthetic complexes and
754 thylakoid membranes during chloroplast biogenesis in *Arabidopsis*. *Plant J* **73**: 250-261
- 755 **Kouřil R, Dekker JP, Boekema EJ** (2012) Supramolecular organization of photosystem II
756 in green plants. *Biochim Biophys Acta* **1817**: 2–12
- 757 **Kreuzwieser J, Scheerer U, Kruse J, Burzlaff T, Honsel A, Alfarraj S, Georgiev P,**
758 **Schnitzler JP, Ghirardo A, Kreuzer I, et al** (2014) The Venus flytrap attracts insects by
759 the release of volatile organic compounds. *J Exp Bot* **65**: 755–66
- 760 **Krumova SB, Laptinok SP, Kovács L, Tóth T, van Hoek A, Garab G, van Amerongen**
761 **H** (2010) Digalactosyl-diacylglycerol-deficiency lowers the thermal stability of thylakoid
762 membranes. *Photosynth Res* **105**: 229–242
- 763 **Labate MT, Ko K, Ko ZW, Pinto LS, Romano MR, Barja PR, Granell A, Friso G, van**
764 **Wijk KJ, Brugnoli E, Labate CA** (2004) Constitutive expression of pea Lhcb 1–2 in
765 tobacco affects plant development, morphology and photosynthetic capacity. *Plant Mol*
766 *Biol* **55**: 701–714
- 767 **Lee AG** (2003) Lipid-protein interactions in biological membranes: a structural perspective.
768 *Biochim Biophys Acta* **1612**: 1-40
- 769 **Lee AG** (2004) How lipids affect the activities of integral membrane proteins, *Biochim*
770 *Biophys Acta* **1666**: 62-87
- 771 **Leister D** (2012) Retrograde signaling in plants: from simple to complex scenarios. *Front*
772 *Plant Sci* **3**: 135
- 773 **Loll B, Kern J, Saenger W, Zouni A, Biesiadka J** (2007) Lipids in Photosystem II:
774 Interactions with protein and cofactors. *Biochim Biophys Acta* **1767**: 509-519
- 775 **Loreto F, Fineschi S** (2014) Reconciling functions and evolution of isoprene emission in
776 higher plants. *New Phytol* doi: 10.1111/nph.13242
- 777 **Loreto F, Schnitzler JP** (2010) Abiotic stresses and induced BVOCs. *Trends Plant Sci* **15**:
778 154-166

- 779 **McLoughlin F, Testerink C** (2013) Phosphatidic acid, a versatile water-stress signal in roots.
780 *Frontiers Plant Sci* **4**, Article 525
- 781 **Mène-Saffrané L, Davoine C, Stolz S, Majcherczyk P, Farmer EE** (2007) Genetic
782 removal of tri-unsaturated fatty acids suppresses developmental and molecular
783 phenotypes of an *Arabidopsis* tocopherol-deficient mutant. Whole-body mapping of
784 malondialdehyde pools in a complex eukaryote. *J Biol Chem* **282**: 35749–35756
- 785 **Mène-Saffrané L, Dubugnon L, Chételat A, Stolz S, Gouhier-Darimont C, Farmer EE**
786 (2009) Nonenzymatic oxidation of trienoic fatty acids contributes to reactive oxygen
787 species management in *Arabidopsis*. *J Biol Chem* **284**: 1702–1708
- 788 **Minagawa J** (2011) State transitions - the molecular remodeling of photosynthetic
789 supercomplexes that controls energy flow in the chloroplast. *Biochim Biophys Acta* **1807**:
790 897–905
- 791 **Müller P, Li X-P, Niyogi KK** (2001) Non-photochemical quenching. A response to excess
792 light energy. *Plant Physiol* **125**: 1558-1566
- 793 **Murchie EH, Niyogi KK** (2011) Manipulation of photoprotection to improve plant
794 photosynthesis. *Plant Physiol* **155**: 86–92
- 795 **Mustárdy L, Buttle K, Steinbach G, Garab G** (2008) The three-dimensional network of
796 the thylakoid membranes in plants: quasihelical model of the granum-stroma assembly.
797 *The Plant Cell* **20**: 2552-2557
- 798 **Nilkens M, Kress E, Lambrev P, Miloslavina Y, Mueller M, Holzwarth AR, Jahns P**
799 (2010) Identification of a slowly inducible zeaxanthin-dependent component of non-
800 photochemical quenching of chlorophyll fluorescence generated under steady-state
801 conditions in *Arabidopsis*. *Biochim Biophys Acta* **1797**: 466–475
- 802 **Oxborough K, Baker NR** (1997) Resolving chlorophyll a fluorescence images of
803 photosynthetic efficiency into photochemical and non-photochemical components
804 calculation of qP and F_v'/F_m' without measuring F_o' . *Photosyn Res* **54**: 135–142
- 805 **Pfannschmidt T** (2010) Plastidial retrograde signaling - a true “plastid factor” or just
806 metabolite signatures? *Trends Plant Sci* **15**: 427-435
- 807 **Porra RJ, Thompson WA, Kriedemann PE** (1989) Determination of accurate extinction
808 coefficients and simultaneous-equations for assaying chlorophyll-a and chlorophyll-b
809 extracted with 4 different solvents—verification of the concentration of chlorophyll
810 standards by atomic-absorption spectroscopy. *Biochim Biophys Acta* **975**: 384–394
- 811 **Pribil M, Labs M, Leister D** (2014) Structure and dynamics of thylakoids in land plants. *J*
812 *Exp Bot* doi:10.1093/jxb/eru090

- 813 **Raghavendra AS, Padmasree K** (2003) Beneficial interactions of mitochondrial
814 metabolism with photosynthetic carbon assimilation. *Trends Plant Sci* **8**: 546-553
- 815 **Ruban AV, Johnson MP, Duffy CDP** (2012) The photoprotective molecular switch in the
816 photosystem II antenna. *Biochim Biophys Acta* **1817**: 167–181
- 817 **Sakurai I, Mizusawa N, Wada H, Sato N** (2007) Digalactosyldiacylglycerol is required for
818 stabilization of the oxygen-evolving complex in photosystem II. *Plant Physiol* **145**: 1361-
819 1370
- 820 **Schmid-Siegert E, Loscos J, Farmer EE** (2012) Inducible malondialdehyde pools in zones
821 of cell proliferation and developing tissues in Arabidopsis. *J Biol Chem* **287**: 8954-8962
- 822 **Sharkey TD, Chen X, Yeh S** (2001) Isoprene increases thermotolerance of fosmidomycin-
823 fed leaves. *Plant Physiol* **125**: 2001–2006
- 824 **Simidjiev I, Barzda V, Mustardy L, Garab G** (1998) Role of thylakoid lipids in the
825 structural flexibility of lamellar aggregates of the isolated light-harvesting chlorophyll a/b
826 complex of photosystem II. *Biochem* **37**: 4169-4173
- 827 **Siwko ME, Marrink SJ, de Vries AH, Kozubek A, Schoot Uiterkamp AJM, Mark AE**
828 (2007) Does isoprene protect plant membranes from thermal shock? A molecular dynamics
829 study. *Biochim Biophys Acta* **1768**: 198–206
- 830 **Testerink C, Munnik T** (2005) Phosphatidic acid: a multifunctional stress signaling lipid in
831 plants. *Trends Plant Sci* **10**: 368- 375
- 832 **Testerink C, Munnik T** (2011) Molecular, cellular, and physiological responses to
833 phosphatidic acid formation in plants. *J Exp Bot* **62**: 2349-2361
- 834 **Teuber M, Zimmer I, Kreuzwieser J, Ache P, Polle A, Rennenberg H, Schnitzler JP**
835 (2008) VOC emissions of Grey poplar leaves as affected by salt stress and different N
836 sources. *Plant Biol* **10**: 86-96
- 837 **Tikkanen M, Nurmi M, Suorsa M, Danielsson R, Mamedov F, Styring S, Aro E-M** (2008)
838 Phosphorylation-dependent regulation of excitation energy distribution between the two
839 photosystems in higher plants, *Biochim Biophys Acta* **1777**: 425-432
- 840 **Vanzo E, Ghirardo A, Merl-Pham J, Lindermayr C, Heller W, Hauck SM, Durner J,**
841 **Schnitzler JP** (2014) S-nitroso-proteome in poplar leaves in response to acute ozone stress.
842 *PLoS One* **9**: e106886
- 843 **Velikova V, Ghirardo A, Vanzo E, Merl J, Hauck SM, Schnitzler JP** (2014) The genetic
844 manipulation of isoprene emissions in poplar plants remodels the chloroplast proteome. *J*
845 *Proteome Res* **13**: 2005-2018

- 846 **Velikova V, Sharkey TD, Loreto F** (2012) Stabilization of thylakoid membranes in
847 isoprene-emitting plants reduces formation of reactive oxygen species. *Plant Signaling &*
848 *Behavior* **7**: 139-141
- 849 **Velikova V, Várkonyi Z, Szabó M, Maslenkova L, Nogues I, Kovács L, Peeva V,**
850 **Busheva M, Garab G, Sharkey TD, Loreto F** (2011) Increased thermostability of
851 thylakoid membranes in isoprene-emitting leaves probed with three biophysical
852 techniques. *Plant Physiol* **157**: 905–916
- 853 **Vickers CE, Gershenzon J, Lerdau MT, Loreto F** (2009) A unified mechanism of action
854 for isoprenoids in plant abiotic stress. *Nat Chem Biol* **5**: 283-291
- 855 **Vidi PA, Kanwischer M, Baginsky S, Austin JR, Csucs G, Dörmann P, Kessler F,**
856 **Bréhélin C** (2006) Tocopherol cyclase (VTE1) localization and vitamin E accumulation
857 in chloroplast plastoglobule lipoprotein particles. *J Biol Chem* **281**: 11225–11234
- 858 **Way DA, Ghirardo A, Kanawati B, Esperschütz J, Monson RK, Jackson RB, Schmitt-**
859 **Kopplin P, Schnitzler JP** (2013) Increasing atmospheric CO₂ reduces metabolic and
860 physiological differences between isoprene and non-isoprene-emitting poplars. *New*
861 *Phytol* **200**: 534-546
- 862 **Weber H, Chételat A, Reymond P, Farmer EE** (2004) Selective and powerful stress gene
863 expression in *Arabidopsis* in response to malondialdehyde. *Plant J* **37**: 877-888
- 864 **Xu J, Chen D, Yan X, Chen J, Zhou C** (2010) Global characterization of the
865 photosynthetic glycerolipids from a marine diatom *Stephanodiscus* sp. by ultra
866 performance liquid chromatography coupled with electrospray ionization-quadrupole-
867 time of flight mass spectrometry. *Anal Chim Acta* **663**: 60-68
- 868 **Yamamoto HY, Higashi RM** (1978) Violaxanthin de-epoxidase. Lipid composition and
869 substrate specificity, *Arch. Bioch. Biophys* **190**: 514-522
- 870 **Yamauchi Y, Furutera A, Seki K, Toyoda Y, Tanaka K, Sugimoto Y** (2008)
871 Malondialdehyde generated from peroxidized linolenic acid causes protein modification
872 in heat-stressed plants. *Plant Physiol Biochem* **46**: 786-793
- 873 **Zaks J, Amarnath K, Sylak-Glassman EJ, Fleming GR** (2013) Models and
874 measurements of energy-dependent quenching. *Photosynth Res* **116**: 389-409
- 875

Table 1. Fatty acid composition ($\mu\text{g mg}^{-1}$ Chl) of the main lipid classes in C_{16} - C_{23} saturated (:0) and unsaturated (:1,:2,:3) compounds in chloroplasts of isoprene emitting (IE, WT/EV) and non emitting (NE, RA1/RA2) poplar plant lines (n16:0, palmitic acid; 16:1, palmitoleic acid; n18:0, stearic acid; 18:1, oleic acid; 18:2, linoleic acid; 18:3, linolenic acid; n23:0, tricosanoic acid).. Fatty acids are designated as the total number of C atoms followed by the number of double bonds and their location (omega) after the colon. Saturated straight-chain fatty acids are indicated by 'n'. Means \pm SE and shown; n=4. Asterisks indicate significant differences with WT; * $P < 0.05$, ** $P < 0.01$, *** $P < 0.001$.

		n16:0	16:1	n18:0	18:1	18:2	18:3	20:3	n23:0
WT	MGDG	21.1 \pm 3.9		2.8 \pm 0.6		61.8 \pm 13.6	411.1 \pm 29.0		
	DGDG	77.5 \pm 22.1		13.2 \pm 5.4		10.7 \pm 3.3	265.1 \pm 17.6	1.4 \pm 0.6	
	Phospholipids	17.7 \pm 3.6	3.5 \pm 1.2	4.1 \pm 0.5	12.9 \pm 4.7	7.6 \pm 1.3	151.9 \pm 16.5		4.0 \pm 1.0
EV	MGDG	19.5 \pm 6.0		2.6 \pm 0.9		54.9 \pm 19.5	350.3 \pm 75.2		
	DGDG	56.0 \pm 15.9		8.7 \pm 2.7		8.8 \pm 3.2	230.3 \pm 59.4	1.0 \pm 0.4	
	Phospholipids	17.8 \pm 2.2	2.4 \pm 0.4	4.3 \pm 0.2	13.8 \pm 6.4	9.1 \pm 0.5	120.9 \pm 3.0		4.1 \pm 1.9
RA1	MGDG	12.7\pm1.7*		1.7 \pm 0.2		38.0\pm8.9*	253.2\pm20.0*		
	DGDG	37.8\pm9.0**		5.7\pm1.5*		5.7\pm1.6*	154.2\pm30.1***	0.5\pm0.2*	
	Phospholipids	9.1 \pm 2.7	1.5 \pm 0.5	3.3 \pm 0.5	3.7 \pm 0.7	5.7 \pm 0.8	66.1\pm9.0*		0.7\pm0.1*
RA2	MGDG	11.9\pm1.1**		1.9 \pm 0.4		35.9\pm4.9*	236.0\pm8.8*		
	DGDG	35.0\pm1.8**		5.4\pm0.4*		4.7\pm0.7*	139.5\pm1.5***	0.5\pm0.1*	
	Phospholipids	11.5\pm1.2*	0.9 \pm 0.3	2.7\pm0.3**	3.6 \pm 1.3	3.2 \pm 0.4	72.6\pm6.6**		2.5 \pm 0.5

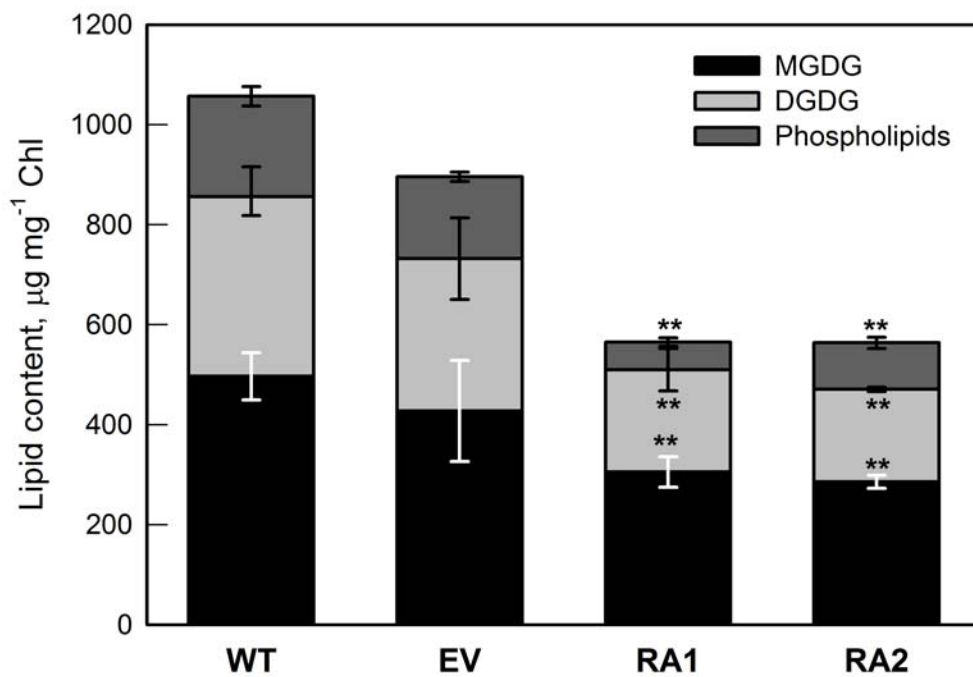


Figure 1. Lipid content in isolated chloroplasts of isoprene emitting (IE, WT/EV) and non-isoprene emitting (NE, RA1/RA2) poplar. Error bars display the SE (n=4). Asterisks indicate significant differences with WT; ** $P < 0.01$.

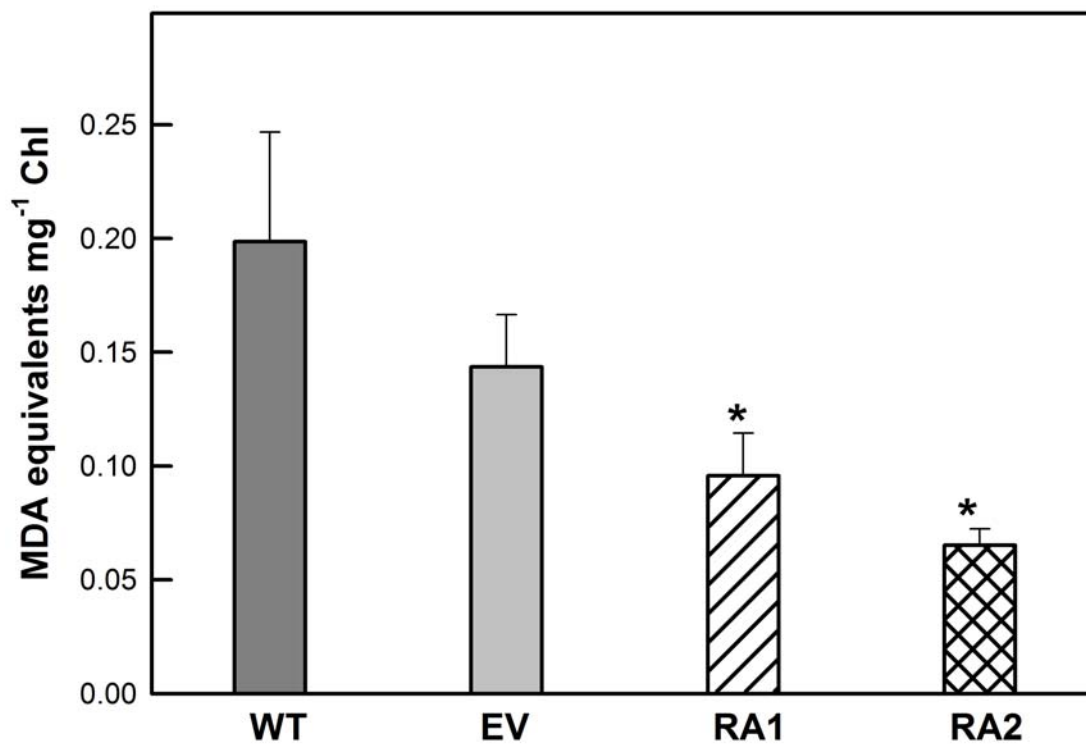


Figure 2. MDA level in isolated chloroplasts of isoprene emitting (IE, WT/EV) and non-isoprene emitting (NE, RA1/RA2) poplar. Error bars display the SE (n=4). Asterisks indicate significant differences with WT; * $P < 0.05$.

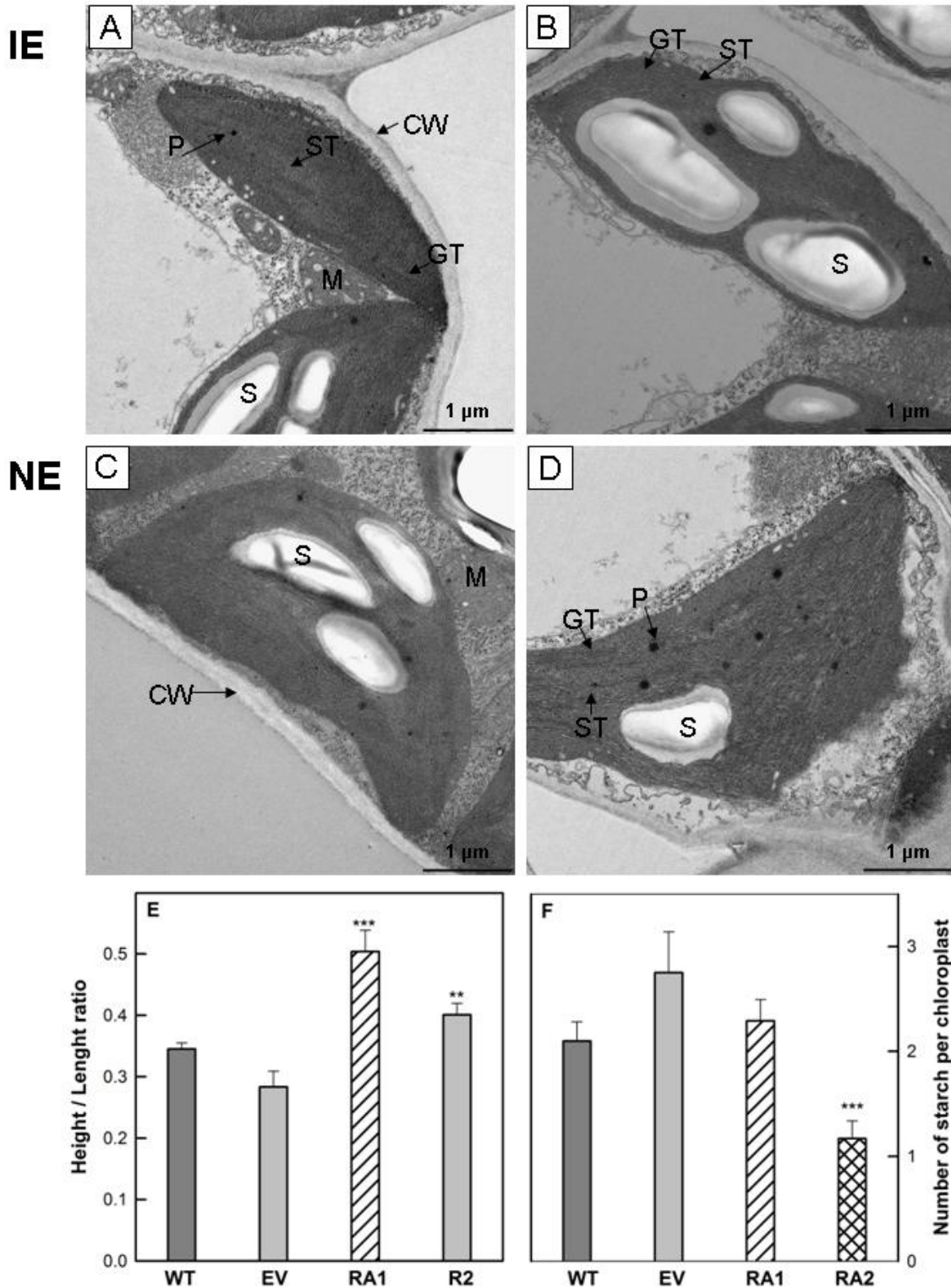


Figure 3. Transmission electron micrographs of representative chloroplast cross-sections taken from the intact leaves of isoprene emitting (IE, WT/EV) (A, B) and non-isoprene emitting (NE, RA1/RA2) (C, D) poplar. Height / Length ratio (E) and average number of starch grains in IE and NE chloroplasts (F). CW - cell wall; GT - granal thylakoids; M, mitochondrion; P, plastoglobuli; S, stroma; SI, starch gain. Scale bar = 1 μ m in A, B, C and D; at x 6,300 magnification.

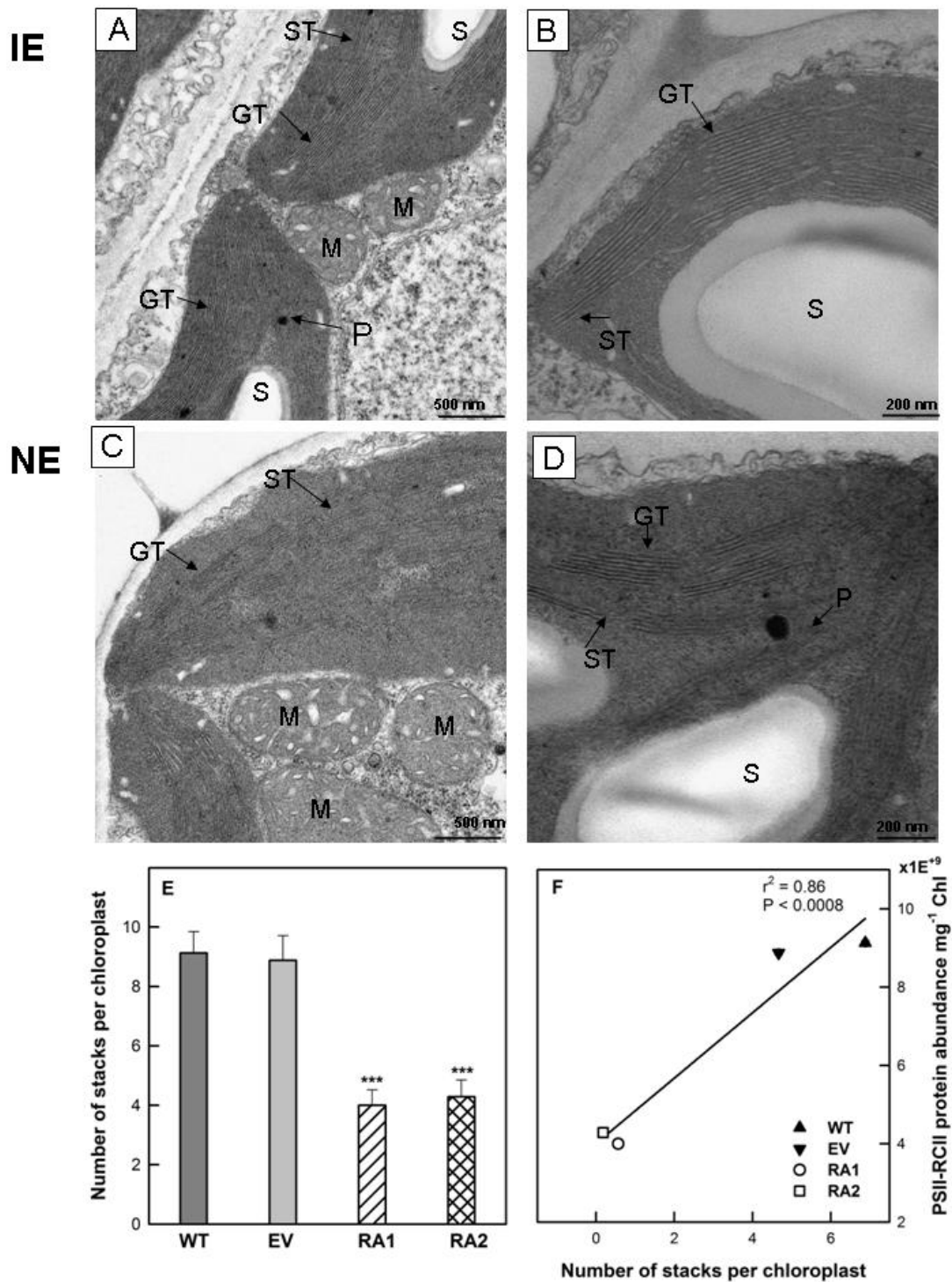


Figure 4. Transmission electron micrographs of representative chloroplast cross-sections taken from the intact leaves of isoprene emitting (IE, WT/EV) (A, B) and non-isoprene emitting (NE, RA1/RA2) (C, D) poplar. Average number of stacks per chloroplast (E) and correlation between PSII – RCII protein abundance (10 peptides; for protein accession numbers see Materials and Methods) and number of stacks (F). CW - cell wall; GT - granal thylakoids; M, mitochondrion; P, plastoglobuli; S, stroma; SI, starch gain. Scale bar = 500 nm in A, and C, at x10,000 magnification; and 200 nm in B and D, at magnification x20,000.

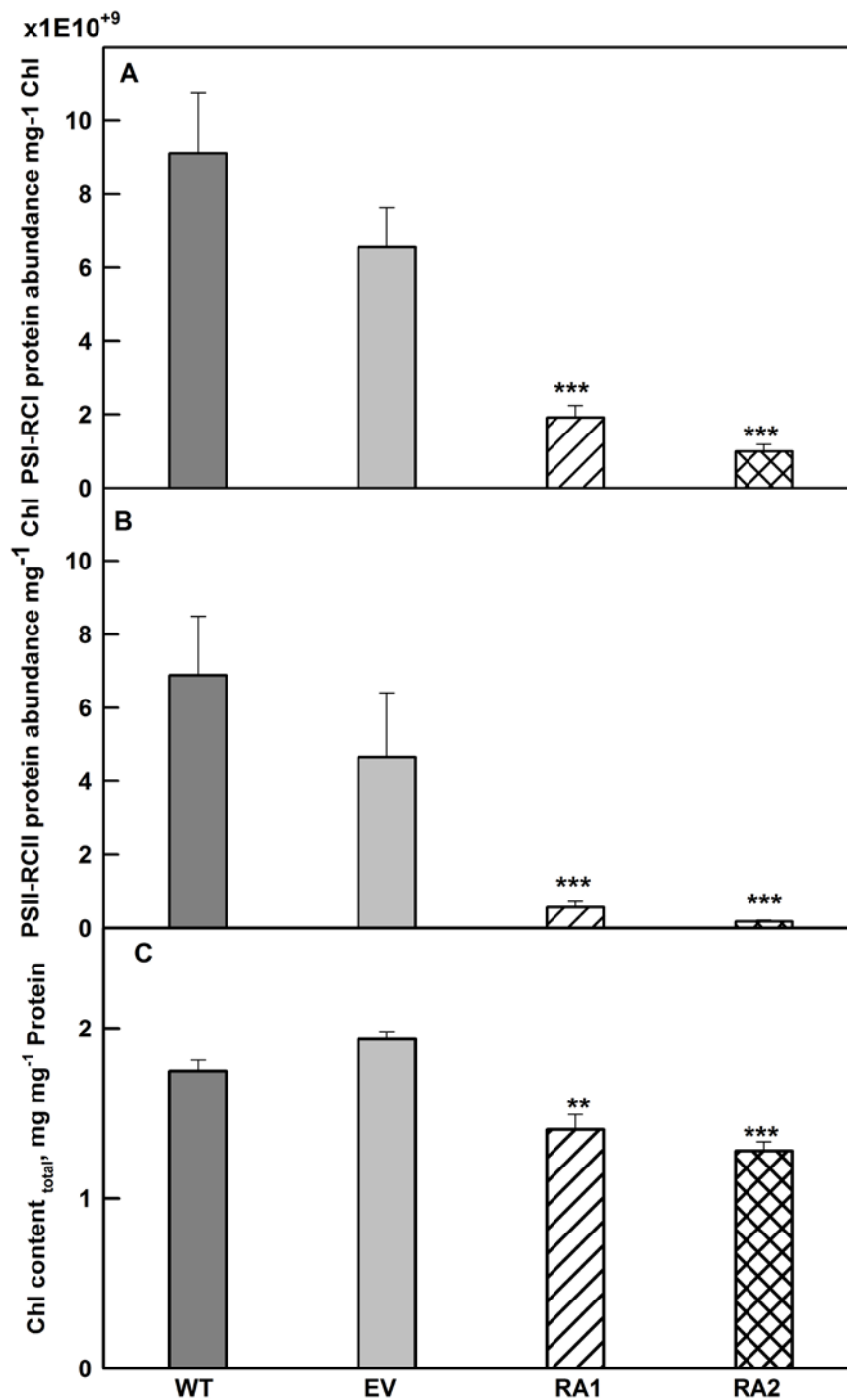


Figure 5. Protein abundance of PSI-RCI (4 peptides; for protein accession numbers see Materials and methods) (A), PSII-RC (10 peptides; for protein accession numbers see Materials and methods) (B) and chlorophyll content (C) in isoprene emitting (IE, WT/EV) and non-isoprene emitting (NE, RA1/RA2) poplar plants. Protein abundance represents sum of MS data extracted from our proteome study (Velikova et al., 2014). Error bars display the SE (n=4). Asterisks indicate significant differences with WT; ** $P < 0.01$; *** $P < 0.001$.

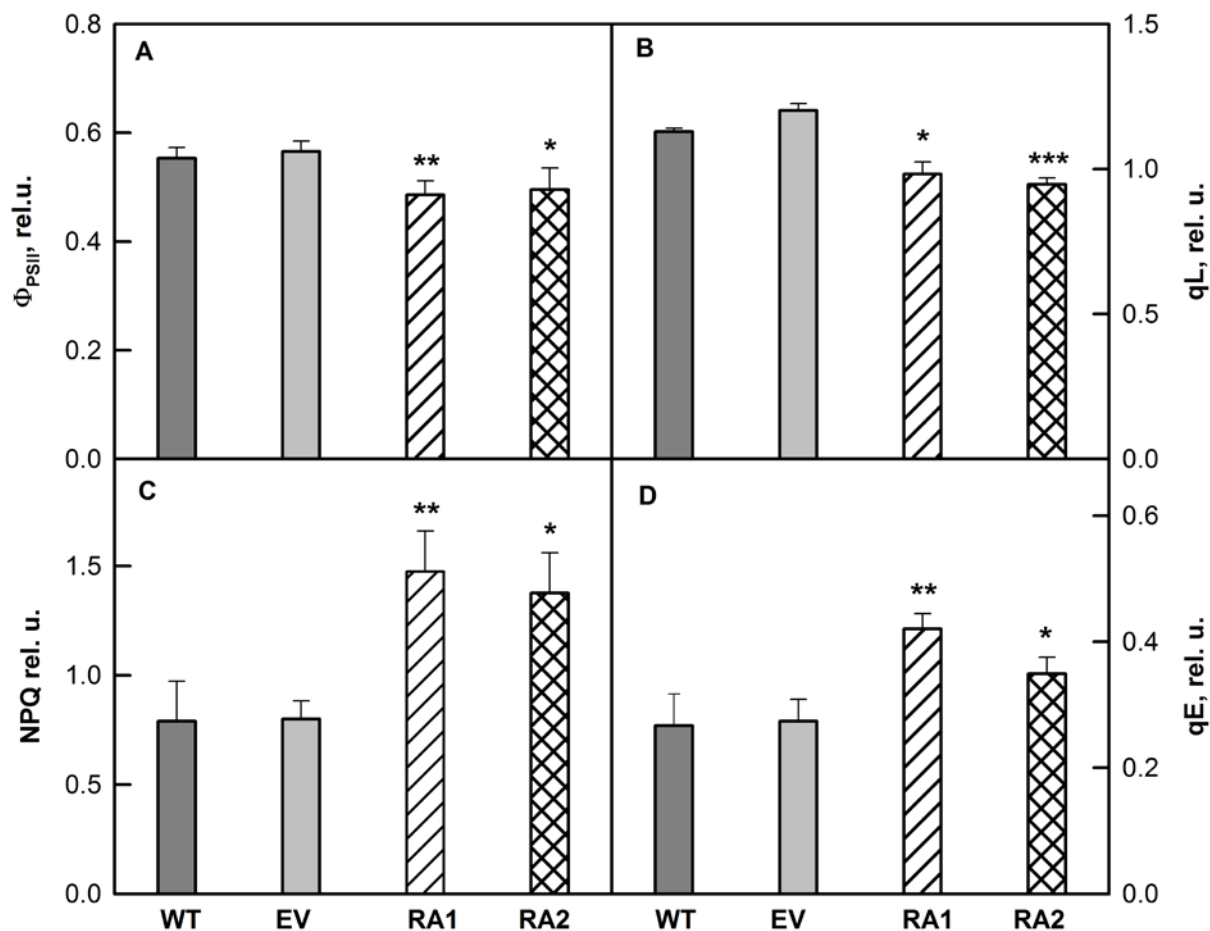


Figure 6. PSII photochemical efficiency (A), redox state of PSII (B), non-photochemical quenching (C) and NPQ energy-dependent component (D) of isoprene emitting (IE, WT/EV) and non-isoprene emitting (NE, RA1/RA2) poplar plants at growth conditions. Values represent means of 5-7 different plants out of three independent experiments ($n = 15-21$, \pm SE is given). Photosynthetic parameters are described in “Material and Methods”. Asterisks indicate significant differences with WT; * $P < 0.05$, ** $P < 0.01$, *** $P < 0.001$.

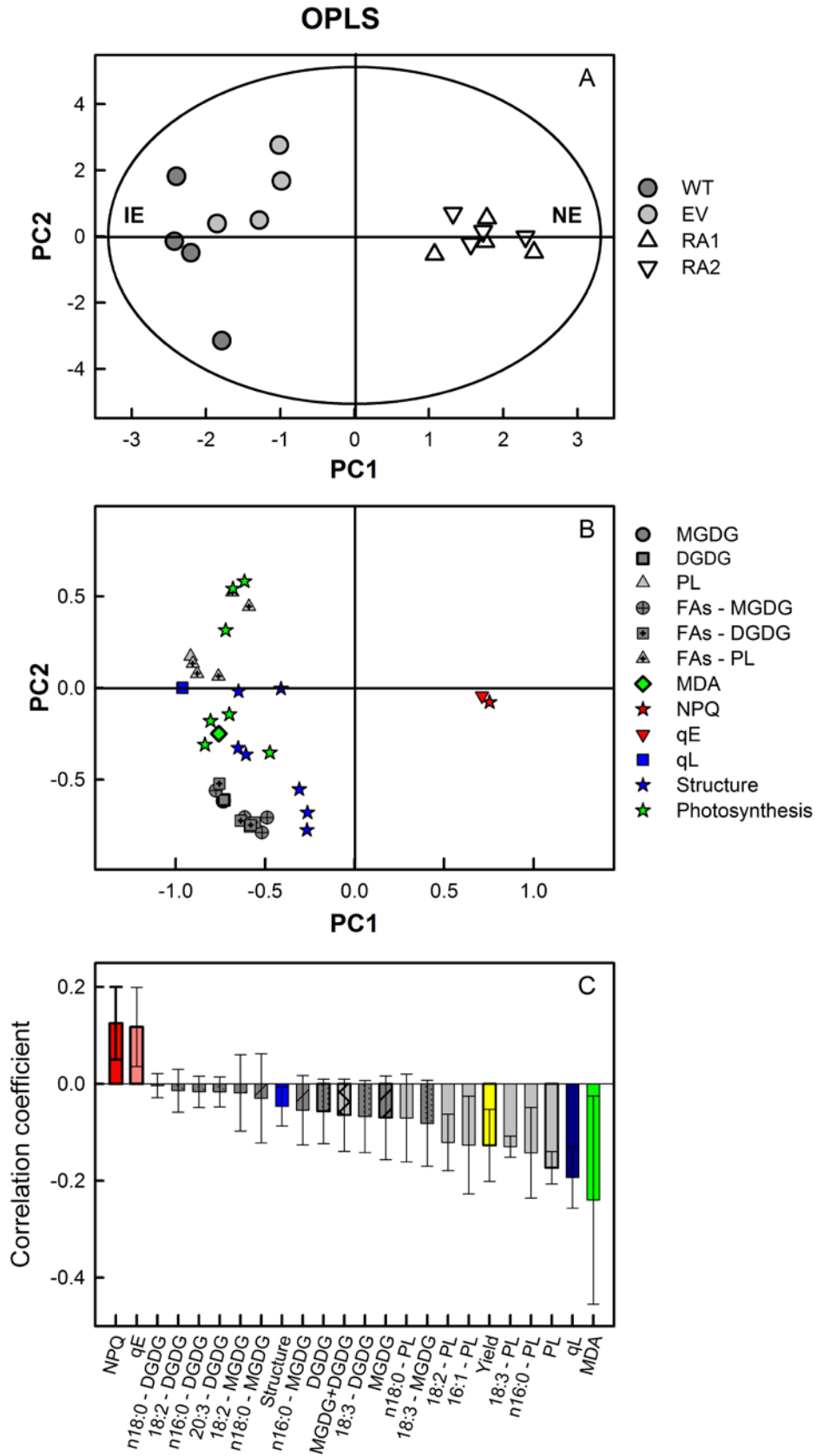


Figure 7. Score (A), loading (B) and correlation coefficient plots (C) of Orthogonal Partial Least Squares (OPLS) of lipid classes, fatty acid composition and MDA contents in isolated chloroplasts, chlorophyll fluorescence parameters measured in intact leaves (NPQ, Φ_{PSII} , qE and qL), and chloroplast proteins related to photosynthesis and proteins with structural activity. (A) IE (WT/EV), grey circles; NE (RA1/RA2), white triangles. (B) Each parameter is indicated with different symbol. Dark grey circles, MGDG; dark gray square, DGDG; gray triangle, PL; dark gray circles with a dot, MGDG – fatty acids; dark gray square with a dot – DGDG – fatty acids; gray triangle with a dot, PL – fatty acids; green diamond, MDA; red star, NPQ; red triangle-down, qE; blue square, qL; blue star, proteins with structural activity; green star, proteins related to photosynthesis. (C) Parameter colors as plot legend B. Only discriminant data with VIP > 1 (for all except proteins) and VIP > 0.5 (proteins) are presented. Model fitness: $Q^2(Y) = 84\%$; $R^2(X) = 44\%$, $R^2 = 93\%$, $R^2(Y) = 100\%$ using one PC; $P = 0.00061$, CV-ANOVA.

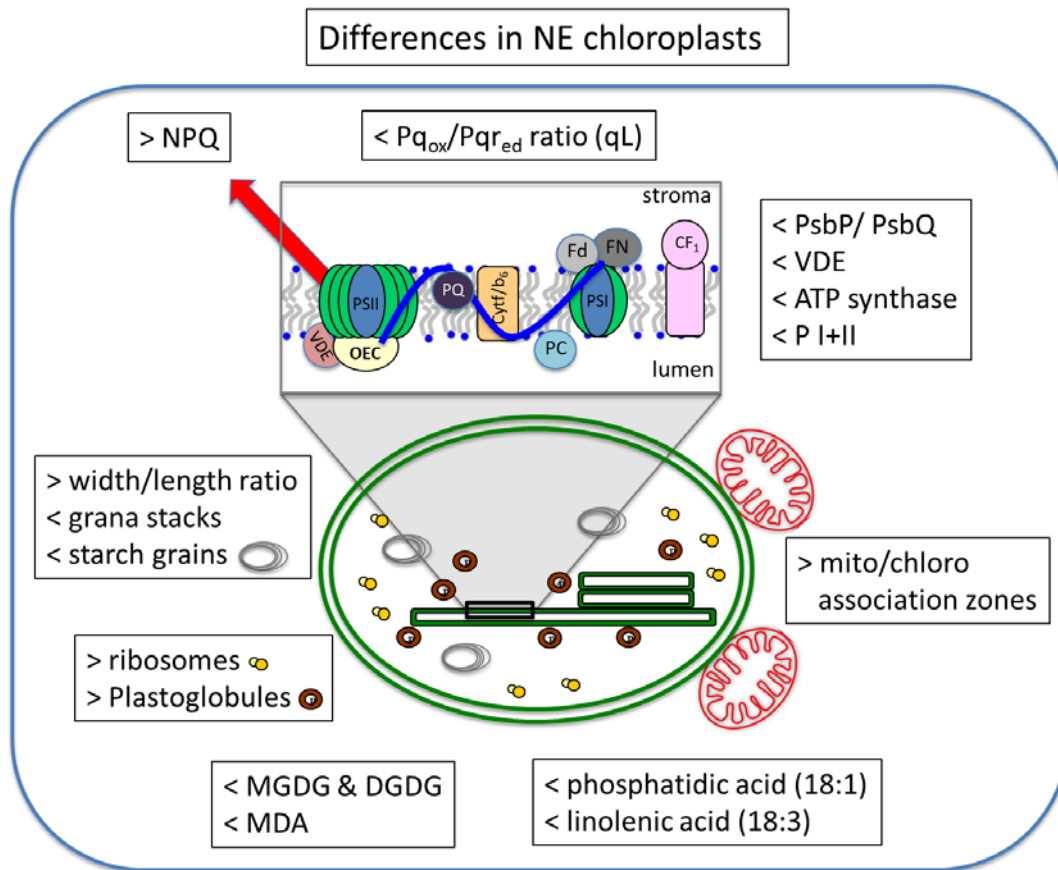


Figure 8. Schematic overview of the changes in chloroplast ultrastructure, lipid composition, change, protein abundance and PSII fluorescence triggered by the suppression of isoprene biosynthesis and emission in poplar plants.

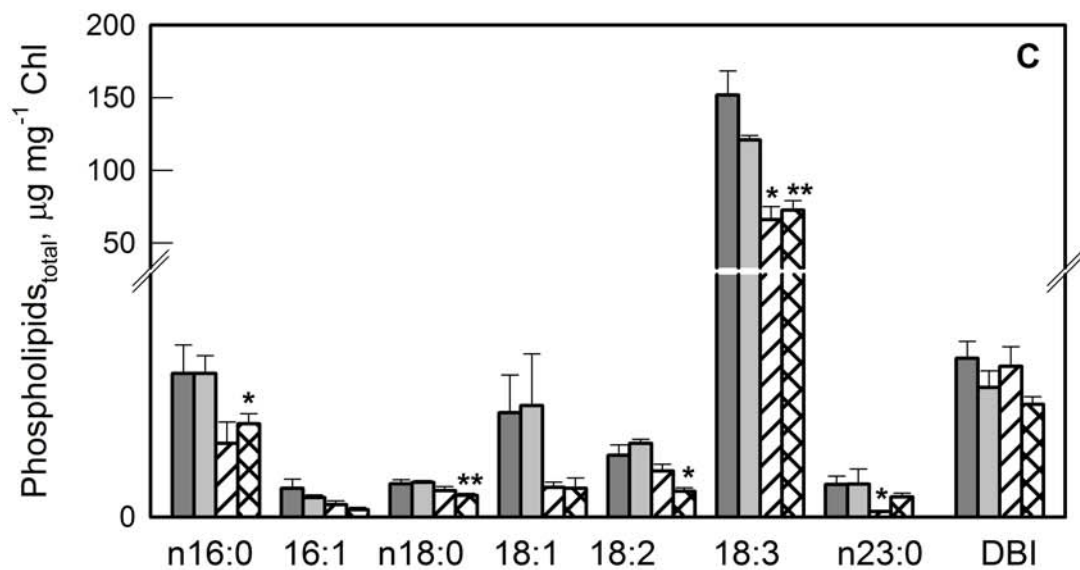
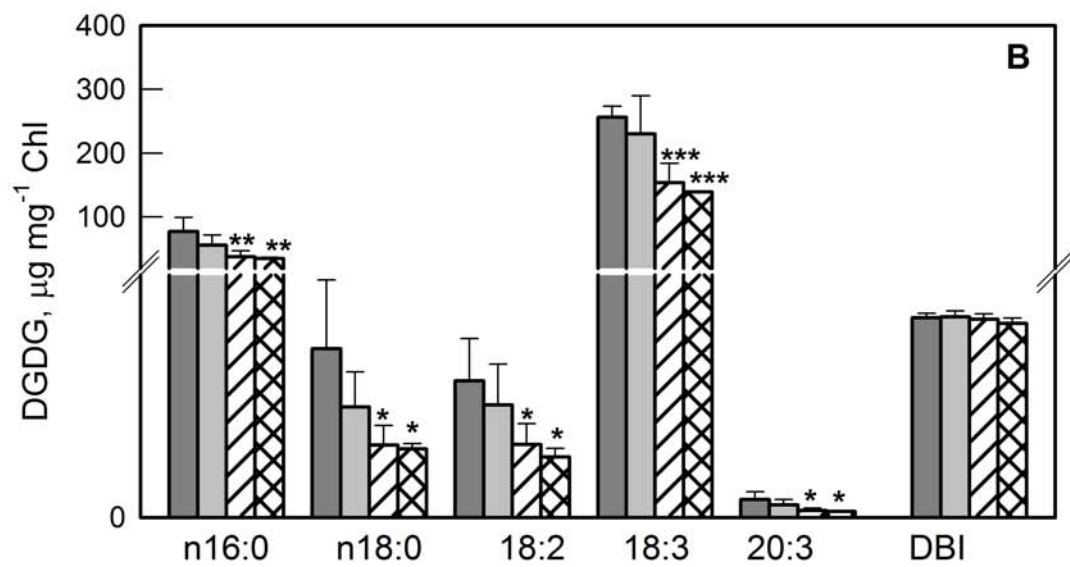
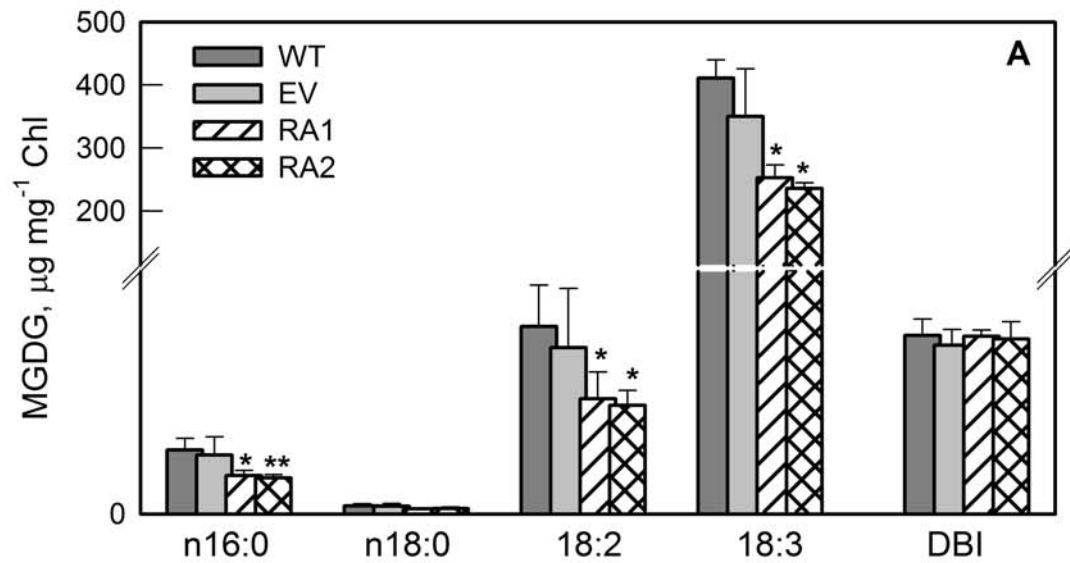


Figure S1. Lipid content and fatty acid composition in isolated chloroplasts of isoprene emitting (IE, WT/EV) and non-emitting (NE, RA1/RA2) poplar. (A) Monogalactosyldiacylglycerols (MGDG), (B) digalactosyldiacylglycerols (DGDG), (C) phospholipids (PL). Error bars display the SE (n=4). Asterisks indicate significant differences with WT; * $P < 0.05$, ** $P < 0.01$, *** $P < 0.001$.

Supplemental Figure 2

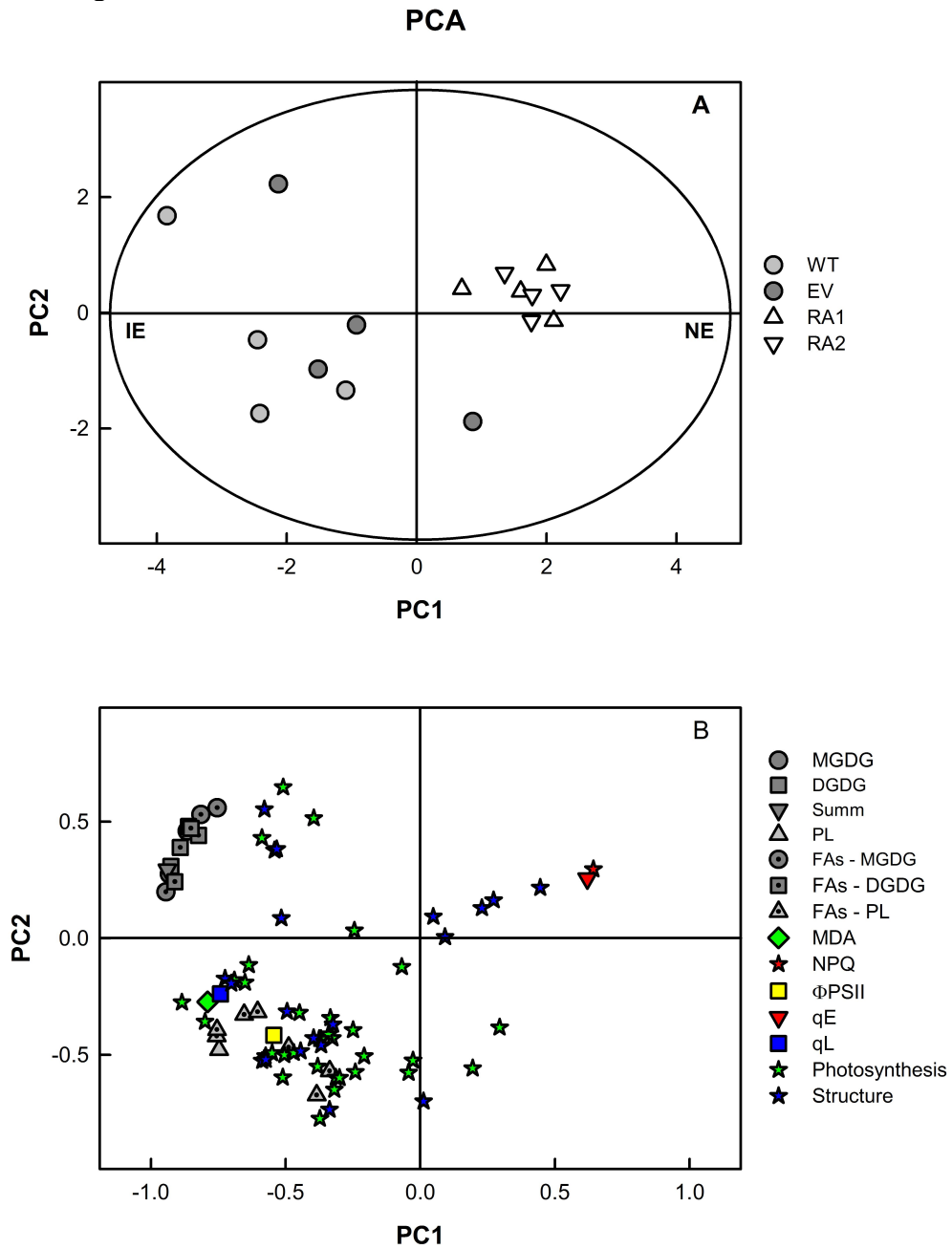


Fig. S2. Score and loading plots of PCA all parameters analyzed (lipid and fatty acid composition, MDA, NPQ, Φ_{PSII} , qE, qL, proteins related to photosynthesis and proteins with structural activity). (A) IE (WT/EV), grey circles; NE (RA1/RA2), white triangles. (B) Each parameter is indicated with different symbol. Dark grey circles, MGDG; dark gray square, DGDG; gray triangle, PL; dark gray circles with a dot, MGDG – fatty acids; dark gray square with a dot – DGDG – fatty acids; gray triangle with a dot, PL – fatty acids; green diamond, MDA; red star, NPQ; red triangle-down, qE; blue square, qL; blue star, proteins with structural activity; green star, proteins related to photosynthesis. Data with VIP > 1 (all data except proteins) and VIP > 0.5 (proteins) are presented.

Parsed Citations

Allen JF, Forsberg J (2001) Molecular recognition in thylakoid structure and function. *Trends Plant Sci* 6: 317-326

Pubmed: [Author and Title](#)

CrossRef: [Author and Title](#)

Google Scholar: [Author Only](#) [Title Only](#) [Author and Title](#)

Austin JR, Frost E, Vidi P-A, Kessler F, Staehelin LA (2006) Plastoglobules are lipoprotein subcompartments of the chloroplast that are permanently coupled to thylakoid membranes and contain biosynthetic enzymes. *Plant Cell* 18: 1693-1703

Pubmed: [Author and Title](#)

CrossRef: [Author and Title](#)

Google Scholar: [Author Only](#) [Title Only](#) [Author and Title](#)

Baker NR (2008) Chlorophyll fluorescence: a probe of photosynthesis in vivo. *Ann Rev Plant Biol* 59: 89-113

Pubmed: [Author and Title](#)

CrossRef: [Author and Title](#)

Google Scholar: [Author Only](#) [Title Only](#) [Author and Title](#)

Behnke K, Ehlting B, Teuber M, Bauerfeind M, Louis S, Hänsch R, Polle A, Bohlmann J, Schnitzler JP (2007) Transgenic, non-isoprene-emitting poplars don't like it hot. *Plant J* 51: 485-499

Pubmed: [Author and Title](#)

CrossRef: [Author and Title](#)

Google Scholar: [Author Only](#) [Title Only](#) [Author and Title](#)

Behnke K, Ghirardo A, Janz D, Kanawati B, Esperschütz J, Zimmer I, Schmitt-Kopplin P, Niinemets Ü, Polle A, Schnitzler JP, Rosenkranz M (2013) Isoprene function in two contrasting poplars under salt and sunflecks. *Tree Physiol* 33: 562-578

Pubmed: [Author and Title](#)

CrossRef: [Author and Title](#)

Google Scholar: [Author Only](#) [Title Only](#) [Author and Title](#)

Behnke K, Kaiser A, Zimmer I, Brüggemann N, Janz D, Polle A, Hampp R, Hänsch R, Popko J, Schmitt-Kopplin P, Ehlting B, Rennenberg H, Barta C, Loreto F, Schnitzler JP (2010a) RNAi-mediated suppression of isoprene emission in poplar impacts phenolic metabolism: a transcriptomic and metabolomic analysis. *Plant Mol Biol* 74: 61-75

Pubmed: [Author and Title](#)

CrossRef: [Author and Title](#)

Google Scholar: [Author Only](#) [Title Only](#) [Author and Title](#)

Behnke K, Kleist E, Uerlings R, Wildt J, Rennenberg H, Schnitzler JP (2009) RNAi-mediated suppression of isoprene biosynthesis in hybrid poplar impacts ozone tolerance. *Tree Physiol* 29: 725-736

Pubmed: [Author and Title](#)

CrossRef: [Author and Title](#)

Google Scholar: [Author Only](#) [Title Only](#) [Author and Title](#)

Behnke K, Loivamäki M, Zimmer I, Rennenberg H, Schnitzler JP, Louis S (2010b) Isoprene emission protects photosynthesis in sunfleck exposed grey poplar. *Photosyn Res* 104: 5-17

Pubmed: [Author and Title](#)

CrossRef: [Author and Title](#)

Google Scholar: [Author Only](#) [Title Only](#) [Author and Title](#)

Bilger W, Björkman O (1991) Temperature dependence of violaxanthin de-epoxidation and non-photochemical fluorescence quenching in intact leaves of *Gossypium hirsutum* L. and *Malva parviflora* L. *Planta* 184: 226-234

Pubmed: [Author and Title](#)

CrossRef: [Author and Title](#)

Google Scholar: [Author Only](#) [Title Only](#) [Author and Title](#)

Bligh EG, Dyer WJ (1959) A rapid method for total lipid extraction and purification. *Can J Biochem Physiol* 37: 911-917

Pubmed: [Author and Title](#)

CrossRef: [Author and Title](#)

Google Scholar: [Author Only](#) [Title Only](#) [Author and Title](#)

Bréhélin C, Kessler F, Wijk KJ (2007) Plastoglobules: versatile lipoprotein particles in plastids. *Trends Plant Sci* 12: 260-266

Pubmed: [Author and Title](#)

CrossRef: [Author and Title](#)

Google Scholar: [Author Only](#) [Title Only](#) [Author and Title](#)

Brilli F, Barta C, Fortunati A, Lerdau M, Loreto F, Centritto M (2007) Response of isoprene emission and carbon metabolism to drought in white poplar (*Populus alba*) saplings. *New Phytol* 175: 244-254

Pubmed: [Author and Title](#)

CrossRef: [Author and Title](#)

Google Scholar: [Author Only](#) [Title Only](#) [Author and Title](#)

Dalton AJ (1955) A chrome-osmium fixative for electron microscopy. *Anat Record* 121: 281

Pubmed: [Author and Title](#)

CrossRef: [Author and Title](#)

Google Scholar: [Author Only](#) [Title Only](#) [Author and Title](#)

Demmig-Adams B, Adams I WW (2006) Photoprotection in an ecological context: the remarkable complexity of thermal energy dissipation. *New Phytol* 172: 11-21

Pubmed: [Author and Title](#)

CrossRef: [Author and Title](#)

Google Scholar: [Author Only](#) [Title Only](#) [Author and Title](#)

Dörmann P, Hoffmann-Benning S, Balbo I, Benning C (1995) Isolation and characterization of an Arabidopsis mutant deficient in the thylakoid lipid digalactosyl diacylglycerol. Plant Cell 7: 1801-1810

Pubmed: [Author and Title](#)

CrossRef: [Author and Title](#)

Google Scholar: [Author Only](#) [Title Only](#) [Author and Title](#)

Eriksson L, Trygg J, Wold S (2008) CV-ANOVA for significance testing of PLS and OPLS models. J Chemom 22: 594-600

Pubmed: [Author and Title](#)

CrossRef: [Author and Title](#)

Google Scholar: [Author Only](#) [Title Only](#) [Author and Title](#)

Esterbauer H, Schaur RJ, Zollner H (1991) Chemistry and biochemistry of 4-hydroxynonenal, malondialdehyde and related aldehydes. Free Radic Biol Med 11: 81-128

Pubmed: [Author and Title](#)

CrossRef: [Author and Title](#)

Google Scholar: [Author Only](#) [Title Only](#) [Author and Title](#)

Fang C, Monson RK, Cowling EB (1996) Isoprene emission, photosynthesis, and growth in sweetgum (*Liquidambar styraciflua*) seedlings exposed to short- and long-term drying cycles. Tree Physiol 16: 441-446

Pubmed: [Author and Title](#)

CrossRef: [Author and Title](#)

Google Scholar: [Author Only](#) [Title Only](#) [Author and Title](#)

Gabashvili IS, Menikh A, Segui J, Fragata M (1998) Protein structure of photosystem II studied by FTIR spectroscopy. Effect of digalactosyldiacylglycerol on the tyrosine side chain residues. J Mol Str 444: 123-133

Pubmed: [Author and Title](#)

CrossRef: [Author and Title](#)

Google Scholar: [Author Only](#) [Title Only](#) [Author and Title](#)

Garab G, Lohner K, Laggner P, Farkas T (2000) Self-regulation of the lipid content of membranes by non-bilayer lipids: a hypothesis. Trends Plant Sci 5: 489-494

Pubmed: [Author and Title](#)

CrossRef: [Author and Title](#)

Google Scholar: [Author Only](#) [Title Only](#) [Author and Title](#)

Garab G, Mustardy L (1999) Role of LHCII-containing macrodomains in the structure, function and dynamics of grana. Aust J Plant Physiol 26: 649-658

Pubmed: [Author and Title](#)

CrossRef: [Author and Title](#)

Google Scholar: [Author Only](#) [Title Only](#) [Author and Title](#)

Genty B, Briantais JM, Baker NR (1989) The relationship between the quantum yield of photosynthetic electron-transport and quenching of chlorophyll fluorescence. Biochim Bioph Acta 990: 87-92

Pubmed: [Author and Title](#)

CrossRef: [Author and Title](#)

Google Scholar: [Author Only](#) [Title Only](#) [Author and Title](#)

Genty B, Goulas Y, Dimon B, Peltier G, Briantais JM, Moya I (1992) Modulation of efficiency of primary conversion in leaves, mechanisms involved at PS2. In: Murata N, ed. Research in photosynthesis, Vol. IV: Proceedings of IXth International Congress on Photosynthesis. Nagoya, Japan, August 30-September 4, 603-610,

Pubmed: [Author and Title](#)

CrossRef: [Author and Title](#)

Google Scholar: [Author Only](#) [Title Only](#) [Author and Title](#)

Ghirardo A, Heller W, Fladung M, Schnitzler JP, Schroeder H (2012) Function of defensive volatiles in pedunculate oak (*Quercus robur*) is tricked by the moth *Tortrix viridana*. Plant Cell Environ 35: 2192-2207

Pubmed: [Author and Title](#)

CrossRef: [Author and Title](#)

Google Scholar: [Author Only](#) [Title Only](#) [Author and Title](#)

Ghirardo A, Sørensen HA, Petersen M, Jacobsen S, Søndergaard I (2005) Early prediction of wheat quality: analysis during grain development using mass spectrometry and multivariate data analysis. Rapid Commun Mass Spectrom 19: 525-532

Pubmed: [Author and Title](#)

CrossRef: [Author and Title](#)

Google Scholar: [Author Only](#) [Title Only](#) [Author and Title](#)

Ghirardo A, Wright LP, Bi Z, Rosenkranz M, Pulido P, Rodríguez-Concepción M, Niinemets Ü, Brüggemann N, Gershenzon J, Schnitzler JP (2014) Metabolic flux analysis of plastidic isoprenoid biosynthesis in poplar leaves emitting and nonemitting isoprene. Plant Physiol 165: 37-51

Pubmed: [Author and Title](#)

CrossRef: [Author and Title](#)

Google Scholar: [Author Only](#) [Title Only](#) [Author and Title](#)

Gounaris K, Barber J (1983) Monogalactosyldiacylglycerol: the most abundant polar lipid in Nature, Trends Biochem Sci 8: 378-381

Pubmed: [Author and Title](#)

CrossRef: [Author and Title](#)

Google Scholar: [Author Only](#) [Title Only](#) [Author and Title](#)

Guenther AB, Jiang X, Heald CL, Sakulyanontvittaya T, Dunlavy D, Edmonds LK, Wang X (2012) The Model of Emissions of Gases and

Aerosols from Nature version 2.1 (MEGAN2.1): an extended and updated framework for modeling biogenic emissions. Geoscientific Model Development 5: 1471-1492

Pubmed: [Author and Title](#)
CrossRef: [Author and Title](#)
Google Scholar: [Author Only Title Only Author and Title](#)

Härtel H, Lokstein H, Dörmann P, Trethewey RN, Benning C (1998) Photosynthetic light utilization and xanthophyll cycle activity in the galactolipid deficient *dgd1* mutant of *Arabidopsis thaliana*. Plant Physiol Biochem 36: 407-417

Pubmed: [Author and Title](#)
CrossRef: [Author and Title](#)
Google Scholar: [Author Only Title Only Author and Title](#)

Hodges DM, DeLong JM, Forney CF, Prange RK (1999) Improving the thiobarbituric acid-reactive-substances assay for estimating lipid peroxidation in plant tissues containing anthocyanin and other interfering compounds. Planta 207: 604-611

Pubmed: [Author and Title](#)
CrossRef: [Author and Title](#)
Google Scholar: [Author Only Title Only Author and Title](#)

Horton P, Wentworth M, Ruban A (2005) Control of the light harvesting function of chloroplast membranes: the LHCII-aggregation model for non-photochemical quenching. FEBS Lett 579: 4201-4206

Pubmed: [Author and Title](#)
CrossRef: [Author and Title](#)
Google Scholar: [Author Only Title Only Author and Title](#)

Horváth I, Glatz A, Nakamoto H, Mishkind ML, Munnik T, Saidi Y, Goloubinoff P, Harwood JL, Vigh L (2012) Heat shock response in photosynthetic organisms: Membrane and lipid connections. Progress Lipid Res 51: 208-220

Pubmed: [Author and Title](#)
CrossRef: [Author and Title](#)
Google Scholar: [Author Only Title Only Author and Title](#)

Ivanov AG, Hendrickson L, Krol M, Selstam E, Öquist G, Hurry V, Huner NPA (2006) Digalactosyl-diacylglycerol deficiency impairs the capacity for photosynthetic intersystem electron transport and state transitions in *Arabidopsis thaliana* due to photosystem I acceptor-side limitations, Plant Cell Physiol 47: 1146-1157

Pubmed: [Author and Title](#)
CrossRef: [Author and Title](#)
Google Scholar: [Author Only Title Only Author and Title](#)

Jacoby RP, Li L, Huang S, Lee CP, Millar AH, Taylor NL (2012) Mitochondrial composition, function and stress response in plants. J Integr Plant Biol 54: 887-906

Pubmed: [Author and Title](#)
CrossRef: [Author and Title](#)
Google Scholar: [Author Only Title Only Author and Title](#)

Jarvis P, Dörmann P, Peto CA, Lutes J, Benning C, Chory J (2000) Galactolipid deficiency and abnormal chloroplast development in the *Arabidopsis* MGD synthase 1 mutant. Proc Natl Acad Sci USA 97: 8175-8179

Pubmed: [Author and Title](#)
CrossRef: [Author and Title](#)
Google Scholar: [Author Only Title Only Author and Title](#)

Joyard J, Ferro M, Masselon C, Seigneurin-Berny D, Salvi D, Garin J, Rolland N (2010) Chloroplast proteomics highlights the subcellular compartmentation of lipid metabolism. Progress in Lipid Research 49: 128-158

Pubmed: [Author and Title](#)
CrossRef: [Author and Title](#)
Google Scholar: [Author Only Title Only Author and Title](#)

Kaling M, Kanawati B, Ghirardo A, Albert A, Winkler JB, Heller W, Barta C, Loreto F, Schmitt-Kopplin P, Schnitzler JP (2015) UV-SI: UV-B mediated metabolic rearrangements in poplar revealed by non-targeted metabolomics. Plant Cell Environ 38: 892-904

Pubmed: [Author and Title](#)
CrossRef: [Author and Title](#)
Google Scholar: [Author Only Title Only Author and Title](#)

Kanervo E, Aro E-M, Murata N (1995) Low unsaturation level of thylakoid membrane lipids limits turnover of the D1 protein of photosystem II at high irradiance. FEBS Lett 364: 239-242

Pubmed: [Author and Title](#)
CrossRef: [Author and Title](#)
Google Scholar: [Author Only Title Only Author and Title](#)

Kirchhoff H, Haase W, Haferkamp S, Schott T, Borinski M, Kubitscheck U, Rögner M (2007) Structural and functional self-organization of photosystem II in grana thylakoids. Biochim Biophys Acta 1767: 1180 -1188

Pubmed: [Author and Title](#)
CrossRef: [Author and Title](#)
Google Scholar: [Author Only Title Only Author and Title](#)

Kirchhoff H, Horstmann S, Weis E (2000) Control of the photosynthetic electron transport by PQ diffusion microdomains in thylakoids of higher plants, Biochim Biophys Acta 1459: 148-168

Pubmed: [Author and Title](#)
CrossRef: [Author and Title](#)
Google Scholar: [Author Only Title Only Author and Title](#)

Kirchhoff H, Mukherjee U, Galla H-J (2002) Molecular architecture of the thylakoid membrane: Lipid diffusion space for

plastoquinone. Biochem 41: 4872-4882

Pubmed: [Author and Title](#)

CrossRef: [Author and Title](#)

Google Scholar: [Author Only](#) [Title Only](#) [Author and Title](#)

Kiss AZ, Ruban AV, Horton P (2008) The PsbS protein controls the organization of the photosystem II antenna in higher plant thylakoid membranes. J Biol Chem 283: 3972-3978

Pubmed: [Author and Title](#)

CrossRef: [Author and Title](#)

Google Scholar: [Author Only](#) [Title Only](#) [Author and Title](#)

Kobayashi K, Narise T, Sonoike K, Hashimoto H, Sato N, Kondo M, Nishimura M, Sato M, Toyooka K, Sugimoto K, Wada H, Masuda T, Ohta H (2013) Role of galactolipid biosynthesis in coordinated development of photosynthetic complexes and thylakoid membranes during chloroplast biogenesis in Arabidopsis. Plant J 73: 250-261

Pubmed: [Author and Title](#)

CrossRef: [Author and Title](#)

Google Scholar: [Author Only](#) [Title Only](#) [Author and Title](#)

Kouril R, Dekker JP, Boekema EJ (2012) Supramolecular organization of photosystem II in green plants. Biochim Biophys Acta 1817: 2-12

Pubmed: [Author and Title](#)

CrossRef: [Author and Title](#)

Google Scholar: [Author Only](#) [Title Only](#) [Author and Title](#)

Kreuzwieser J, Scheerer U, Kruse J, Burzlaff T, Honsel A, Alfarraj S, Georgiev P, Schnitzler JP, Ghirardo A, Kreuzer I, et al (2014) The Venus flytrap attracts insects by the release of volatile organic compounds. J Exp Bot 65: 755-66

Pubmed: [Author and Title](#)

CrossRef: [Author and Title](#)

Google Scholar: [Author Only](#) [Title Only](#) [Author and Title](#)

Krumova SB, Laptinok SP, Kovács L, Tóth T, van Hoek A, Garab G, van Amerongen H (2010) Digalactosyl-diacylglycerol-deficiency lowers the thermal stability of thylakoid membranes. Photosynth Res 105: 229-242

Pubmed: [Author and Title](#)

CrossRef: [Author and Title](#)

Google Scholar: [Author Only](#) [Title Only](#) [Author and Title](#)

Labate MT, Ko K, Ko ZW, Pinto LS, Romano MR, Barja PR, Granell A, Friso G, van Wijk KJ, Brugnoli E, Labate CA (2004) Constitutive expression of pea Lhcb 1-2 in tobacco affects plant development, morphology and photosynthetic capacity. Plant Mol Biol 55: 701-714

Pubmed: [Author and Title](#)

CrossRef: [Author and Title](#)

Google Scholar: [Author Only](#) [Title Only](#) [Author and Title](#)

Lee AG (2003) Lipid-protein interactions in biological membranes: a structural perspective. Biochim Biophys Acta 1612: 1-40

Pubmed: [Author and Title](#)

CrossRef: [Author and Title](#)

Google Scholar: [Author Only](#) [Title Only](#) [Author and Title](#)

Lee AG (2004) How lipids affect the activities of integral membrane proteins, Biochim Biophys Acta 1666: 62-87

Pubmed: [Author and Title](#)

CrossRef: [Author and Title](#)

Google Scholar: [Author Only](#) [Title Only](#) [Author and Title](#)

Leister D (2012) Retrograde signaling in plants: from simple to complex scenarios. Front Plant Sci 3: 135

Pubmed: [Author and Title](#)

CrossRef: [Author and Title](#)

Google Scholar: [Author Only](#) [Title Only](#) [Author and Title](#)

Loll B, Kern J, Saenger W, Zouni A, Biesiadka J (2007) Lipids in Photosystem II: Interactions with protein and cofactors. Biochim Biophys Acta 1767: 509-519

Pubmed: [Author and Title](#)

CrossRef: [Author and Title](#)

Google Scholar: [Author Only](#) [Title Only](#) [Author and Title](#)

Loreto F, Fineschi S (2014) Reconciling functions and evolution of isoprene emission in higher plants. New Phytol doi: 10.1111/nph.13242

Pubmed: [Author and Title](#)

CrossRef: [Author and Title](#)

Google Scholar: [Author Only](#) [Title Only](#) [Author and Title](#)

Loreto F, Schnitzler JP (2010) Abiotic stresses and induced BVOCs. Trends Plant Sci 15: 154-166

Pubmed: [Author and Title](#)

CrossRef: [Author and Title](#)

Google Scholar: [Author Only](#) [Title Only](#) [Author and Title](#)

McLoughlin F, Testerink C (2013) Phosphatidic acid, a versatile water-stress signal in roots. Frontiers Plant Sci 4, Article 525

Pubmed: [Author and Title](#)

CrossRef: [Author and Title](#)

Google Scholar: [Author Only](#) [Title Only](#) [Author and Title](#)

Mène-Safrané L, Davoine C, Stolz S, Mejhersczyk P, Farmer EE (2007) Genetic removal of tri-unsaturated fatty acids suppresses

developmental and molecular phenotypes of an Arabidopsis tocopherol-deficient mutant. Whole-body mapping of malondialdehyde pools in a complex eukaryote. J Biol Chem 282: 35749-35756

Pubmed: [Author and Title](#)
CrossRef: [Author and Title](#)
Google Scholar: [Author Only](#) [Title Only](#) [Author and Title](#)

Mène-Safrané L, Dubugnon L, Chételat A, Stolz S, Gouhier-Darimont C, Farmer EE (2009) Nonenzymatic oxidation of trienoic fatty acids contributes to reactive oxygen species management in Arabidopsis. J Biol Chem 284: 1702-1708

Pubmed: [Author and Title](#)
CrossRef: [Author and Title](#)
Google Scholar: [Author Only](#) [Title Only](#) [Author and Title](#)

Minagawa J (2011) State transitions - the molecular remodeling of photosynthetic supercomplexes that controls energy flow in the chloroplast. Biochim Biophys Acta 1807: 897-905

Pubmed: [Author and Title](#)
CrossRef: [Author and Title](#)
Google Scholar: [Author Only](#) [Title Only](#) [Author and Title](#)

Müller P, Li X-P, Niyogi KK (2001) Non-photochemical quenching. A response to excess light energy. Plant Physiol 125: 1558-1566

Pubmed: [Author and Title](#)
CrossRef: [Author and Title](#)
Google Scholar: [Author Only](#) [Title Only](#) [Author and Title](#)

Murchie EH, Niyogi KK (2011) Manipulation of photoprotection to improve plant photosynthesis. Plant Physiol 155: 86-92

Pubmed: [Author and Title](#)
CrossRef: [Author and Title](#)
Google Scholar: [Author Only](#) [Title Only](#) [Author and Title](#)

Mustárdy L, Buttler K, Steinbach G, Garab G (2008) The three-dimensional network of the thylakoid membranes in plants: quasi-helical model of the granum-stroma assembly. The Plant Cell 20: 2552-2557

Pubmed: [Author and Title](#)
CrossRef: [Author and Title](#)
Google Scholar: [Author Only](#) [Title Only](#) [Author and Title](#)

Nilkens M, Kress E, Lambrev P, Miloslavina Y, Mueller M, Holzwarth AR, Jahns P (2010) Identification of a slowly inducible zeaxanthin-dependent component of non-photochemical quenching of chlorophyll fluorescence generated under steady-state conditions in Arabidopsis. Biochim Biophys Acta 1797: 466-475

Pubmed: [Author and Title](#)
CrossRef: [Author and Title](#)
Google Scholar: [Author Only](#) [Title Only](#) [Author and Title](#)

Oxborough K, Baker NR (1997) Resolving chlorophyll a fluorescence images of photosynthetic efficiency into photochemical and non-photochemical components calculation of qP and Fv'/Fm' without measuring Fo'. Photosyn Res 54: 135-142

Pubmed: [Author and Title](#)
CrossRef: [Author and Title](#)
Google Scholar: [Author Only](#) [Title Only](#) [Author and Title](#)

Pfannschmidt T (2010) Plastidial retrograde signaling - a true "plastid factor" or just metabolite signatures? Trends Plant Sci 15: 427-435

Pubmed: [Author and Title](#)
CrossRef: [Author and Title](#)
Google Scholar: [Author Only](#) [Title Only](#) [Author and Title](#)

Porra RJ, Thompson WA, Kriedemann PE (1989) Determination of accurate extinction coefficients and simultaneous-equations for assaying chlorophyll-a and chlorophyll-b extracted with 4 different solvents—verification of the concentration of chlorophyll standards by atomic-absorption spectroscopy. Biochim Biophys Acta 975: 384-394

Pubmed: [Author and Title](#)
CrossRef: [Author and Title](#)
Google Scholar: [Author Only](#) [Title Only](#) [Author and Title](#)

Pribil M, Labs M, Leister D (2014) Structure and dynamics of thylakoids in land plants. J Exp Bot doi:10.1093/jxb/eru090

Pubmed: [Author and Title](#)
CrossRef: [Author and Title](#)
Google Scholar: [Author Only](#) [Title Only](#) [Author and Title](#)

Raghavendra AS, Padmasree K (2003) Beneficial interactions of mitochondrial metabolism with photosynthetic carbon assimilation. Trends Plant Sci 8: 546-553

Pubmed: [Author and Title](#)
CrossRef: [Author and Title](#)
Google Scholar: [Author Only](#) [Title Only](#) [Author and Title](#)

Ruban AV, Johnson MP, Duffy CDP (2012) The photoprotective molecular switch in the photosystem II antenna. Biochim Biophys Acta 1817: 167-181

Pubmed: [Author and Title](#)
CrossRef: [Author and Title](#)
Google Scholar: [Author Only](#) [Title Only](#) [Author and Title](#)

Sakurai I, Mizusawa N, Wada H, Sato N (2007) Digalactosyldiacylglycerol is required for stabilization of the oxygen-evolving complex in photosystem II. Plant Physiol 145: 1361-1370

Pubmed: [Author and Title](#)

CrossRef: [Author and Title](#)
Google Scholar: [Author Only Title Only Author and Title](#)

Schmid-Siegert E, Loscos J, Farmer EE (2012) Inducible malondialdehyde pools in zones of cell proliferation and developing tissues in Arabidopsis. J Biol Chem 287: 8954-8962

Pubmed: [Author and Title](#)
CrossRef: [Author and Title](#)
Google Scholar: [Author Only Title Only Author and Title](#)

Sharkey TD, Chen X, Yeh S (2001) Isoprene increases thermotolerance of fosmidomycin-fed leaves. Plant Physiol 125: 2001-2006

Pubmed: [Author and Title](#)
CrossRef: [Author and Title](#)
Google Scholar: [Author Only Title Only Author and Title](#)

Simidjiev I, Barzda V, Mustardy L, Garab G (1998) Role of thylakoid lipids in the structural flexibility of lamellar aggregates of the isolated light-harvesting chlorophyll a/b complex of photosystem II. Biochem 37: 4169-4173

Pubmed: [Author and Title](#)
CrossRef: [Author and Title](#)
Google Scholar: [Author Only Title Only Author and Title](#)

Siwko ME, Marrink SJ, de Vries AH, Kozubek A, Schoot Uiterkamp AJM, Mark AE (2007) Does isoprene protect plant membranes from thermal shock? A molecular dynamics study. Biochim Biophys Acta 1768: 198-206

Pubmed: [Author and Title](#)
CrossRef: [Author and Title](#)
Google Scholar: [Author Only Title Only Author and Title](#)

Testerink C, Munnik T (2005) Phosphatidic acid: a multifunctional stress signaling lipid in plants. Trends Plant Sci 10: 368- 375

Pubmed: [Author and Title](#)
CrossRef: [Author and Title](#)
Google Scholar: [Author Only Title Only Author and Title](#)

Testerink C, Munnik T (2011) Molecular, cellular, and physiological responses to phosphatidic acid formation in plants. J Exp Bot 62: 2349-2361

Pubmed: [Author and Title](#)
CrossRef: [Author and Title](#)
Google Scholar: [Author Only Title Only Author and Title](#)

Teuber M, Zimmer I, Kreuzwieser J, Ache P, Polle A, Rennenberg H, Schnitzler JP (2008) VOC emissions of Grey poplar leaves as affected by salt stress and different N sources. Plant Biol 10: 86-96

Pubmed: [Author and Title](#)
CrossRef: [Author and Title](#)
Google Scholar: [Author Only Title Only Author and Title](#)

Tikkanen M, Nurmi M, Suorsa M, Danielsson R, Mamedov F, Styring S, Aro E-M (2008) Phosphorylation-dependent regulation of excitation energy distribution between the two photosystems in higher plants, Biochim Biophys Acta 1777: 425-432

Pubmed: [Author and Title](#)
CrossRef: [Author and Title](#)
Google Scholar: [Author Only Title Only Author and Title](#)

Vanzo E, Ghirardo A, Merl-Pham J, Lindermayr C, Heller W, Hauck SM, Durner J, Schnitzler JP (2014) S-nitroso-proteome in poplar leaves in response to acute ozone stress. PLoS One 9: e106886

Pubmed: [Author and Title](#)
CrossRef: [Author and Title](#)
Google Scholar: [Author Only Title Only Author and Title](#)

Velikova V, Ghirardo A, Vanzo E, Merl J, Hauck SM, Schnitzler JP (2014) The genetic manipulation of isoprene emissions in poplar plants remodels the chloroplast proteome. J Proteome Res 13: 2005-2018

Pubmed: [Author and Title](#)
CrossRef: [Author and Title](#)
Google Scholar: [Author Only Title Only Author and Title](#)

Velikova V, Sharkey TD, Loreto F (2012) Stabilization of thylakoid membranes in isoprene-emitting plants reduces formation of reactive oxygen species. Plant Signaling & Behavior 7: 139-141

Pubmed: [Author and Title](#)
CrossRef: [Author and Title](#)
Google Scholar: [Author Only Title Only Author and Title](#)

Velikova V, Várkonyi Z, Szabó M, Maslenskova L, Noguez I, Kovács L, Peeva V, Busheva M, Garab G, Sharkey TD, Loreto F (2011) Increased thermostability of thylakoid membranes in isoprene-emitting leaves probed with three biophysical techniques. Plant Physiol 157: 905-916

Pubmed: [Author and Title](#)
CrossRef: [Author and Title](#)
Google Scholar: [Author Only Title Only Author and Title](#)

Vickers CE, Gershenzon J, Lerdau MT, Loreto F (2009) A unified mechanism of action for isoprenoids in plant abiotic stress. Nat Chem Biol 5: 283-291

Pubmed: [Author and Title](#)
CrossRef: [Author and Title](#)
Google Scholar: [Author Only Title Only Author and Title](#)

Vidi PA, Kanwischer M, Baginsky S, Austin JR, Csucs G, Dörmann P, Kessler F, Bréhélin G (2006) Tocopherol cyclase (VTE1)

Localization and vitamin E accumulation in chloroplast plastoglobule lipoprotein particles. J Biol Chem 281: 11225-11234

Pubmed: [Author and Title](#)

CrossRef: [Author and Title](#)

Google Scholar: [Author Only](#) [Title Only](#) [Author and Title](#)

Way DA, Ghirardo A, Kanawati B, Esperschütz J, Monson RK, Jackson RB, Schmitt-Kopplin P, Schnitzler JP (2013) Increasing atmospheric CO₂ reduces metabolic and physiological differences between isoprene and non-isoprene-emitting poplars. New Phytol 200: 534-546

Pubmed: [Author and Title](#)

CrossRef: [Author and Title](#)

Google Scholar: [Author Only](#) [Title Only](#) [Author and Title](#)

Weber H, Chételat A, Reymond P, Farmer EE (2004) Selective and powerful stress gene expression in Arabidopsis in response to malondialdehyde. Plant J 37: 877-888

Pubmed: [Author and Title](#)

CrossRef: [Author and Title](#)

Google Scholar: [Author Only](#) [Title Only](#) [Author and Title](#)

Xu J, Chen D, Yan X, Chen J, Zhou C (2010) Global characterization of the photosynthetic glycerolipids from a marine diatom *Stephanodiscus* sp. by ultra performance liquid chromatography coupled with electrospray ionization-quadrupole-time of flight mass spectrometry. Anal Chim Acta 663: 60-68

Pubmed: [Author and Title](#)

CrossRef: [Author and Title](#)

Google Scholar: [Author Only](#) [Title Only](#) [Author and Title](#)

Yamamoto HY, Higashi RM (1978) Violaxanthin de-epoxidase. Lipid composition and substrate specificity, Arch. Bioch. Biophys 190: 514-522

Pubmed: [Author and Title](#)

CrossRef: [Author and Title](#)

Google Scholar: [Author Only](#) [Title Only](#) [Author and Title](#)

Yamauchi Y, Furutera A, Seki K, Toyoda Y, Tanaka K, Sugimoto Y (2008) Malondialdehyde generated from peroxidized linolenic acid causes protein modification in heat-stressed plants. Plant Physiol Biochem 46: 786-793

Pubmed: [Author and Title](#)

CrossRef: [Author and Title](#)

Google Scholar: [Author Only](#) [Title Only](#) [Author and Title](#)

Zaks J, Amarnath K, Sylak-Glassman EJ, Fleming GR (2013) Models and measurements of energy-dependent quenching. Photosynth Res 116: 389-409

Pubmed: [Author and Title](#)

CrossRef: [Author and Title](#)

Google Scholar: [Author Only](#) [Title Only](#) [Author and Title](#)

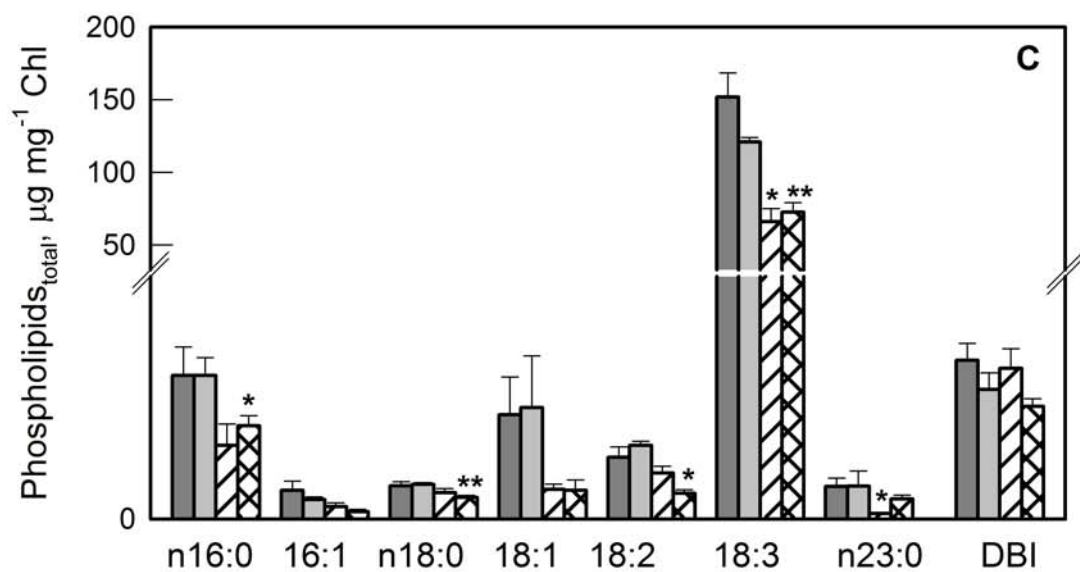
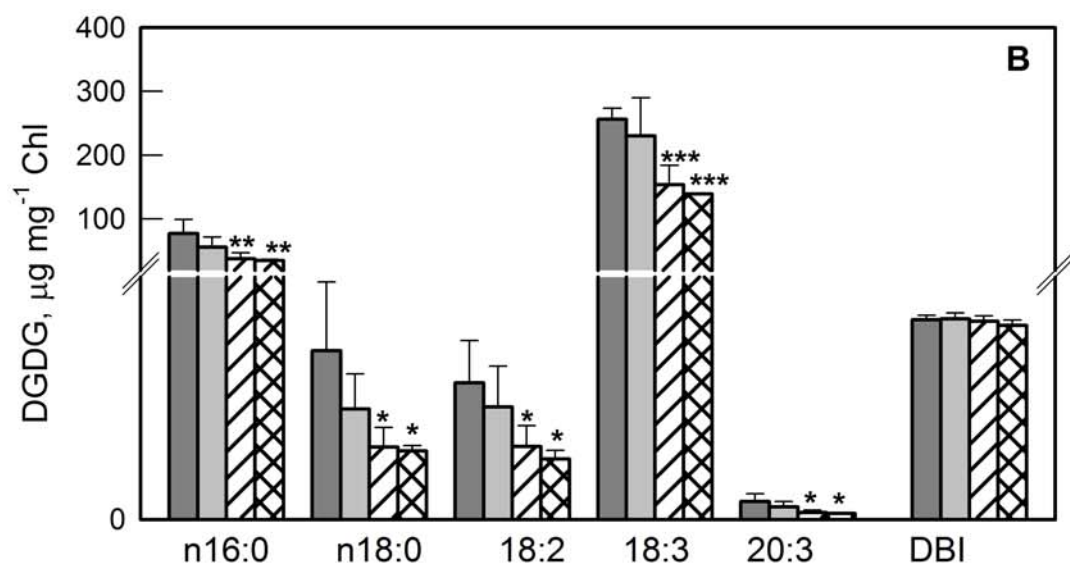
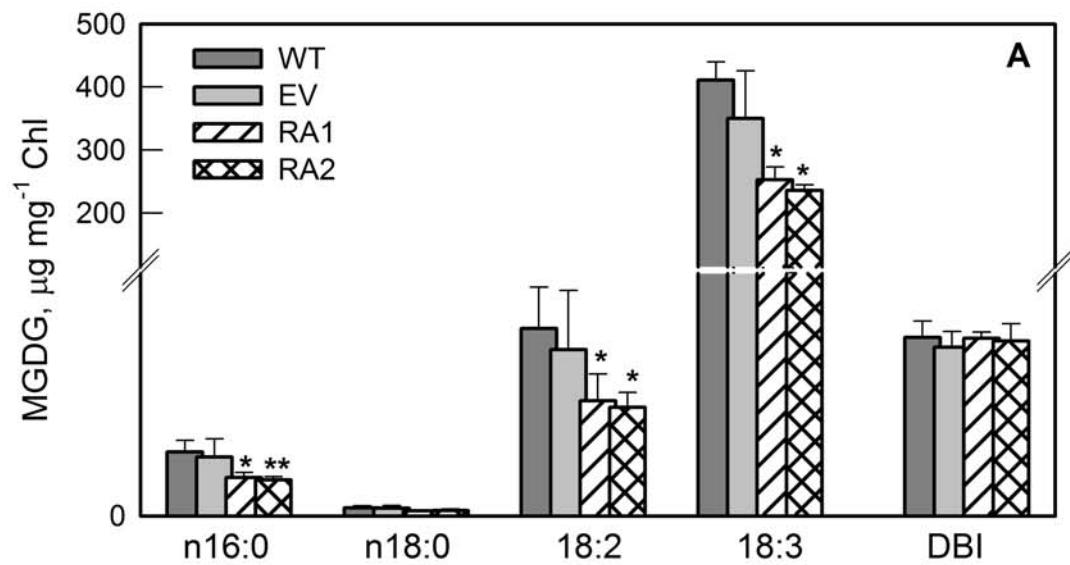


Figure S1. Lipid content and fatty acid composition in isolated chloroplasts of isoprene emitting (IE, WT/EV) and non-emitting (NE, RA1/RA2) poplar. (A) Monogalactosyldiacylglycerols (MGDG), (B) digalactosyldiacylglycerols (DGDG), (C) phospholipids (PL). Error bars display the SE (n=4). Asterisks indicate significant differences with WT; * $P < 0.05$, ** $P < 0.01$, *** $P < 0.001$.

Supplemental Figure 2

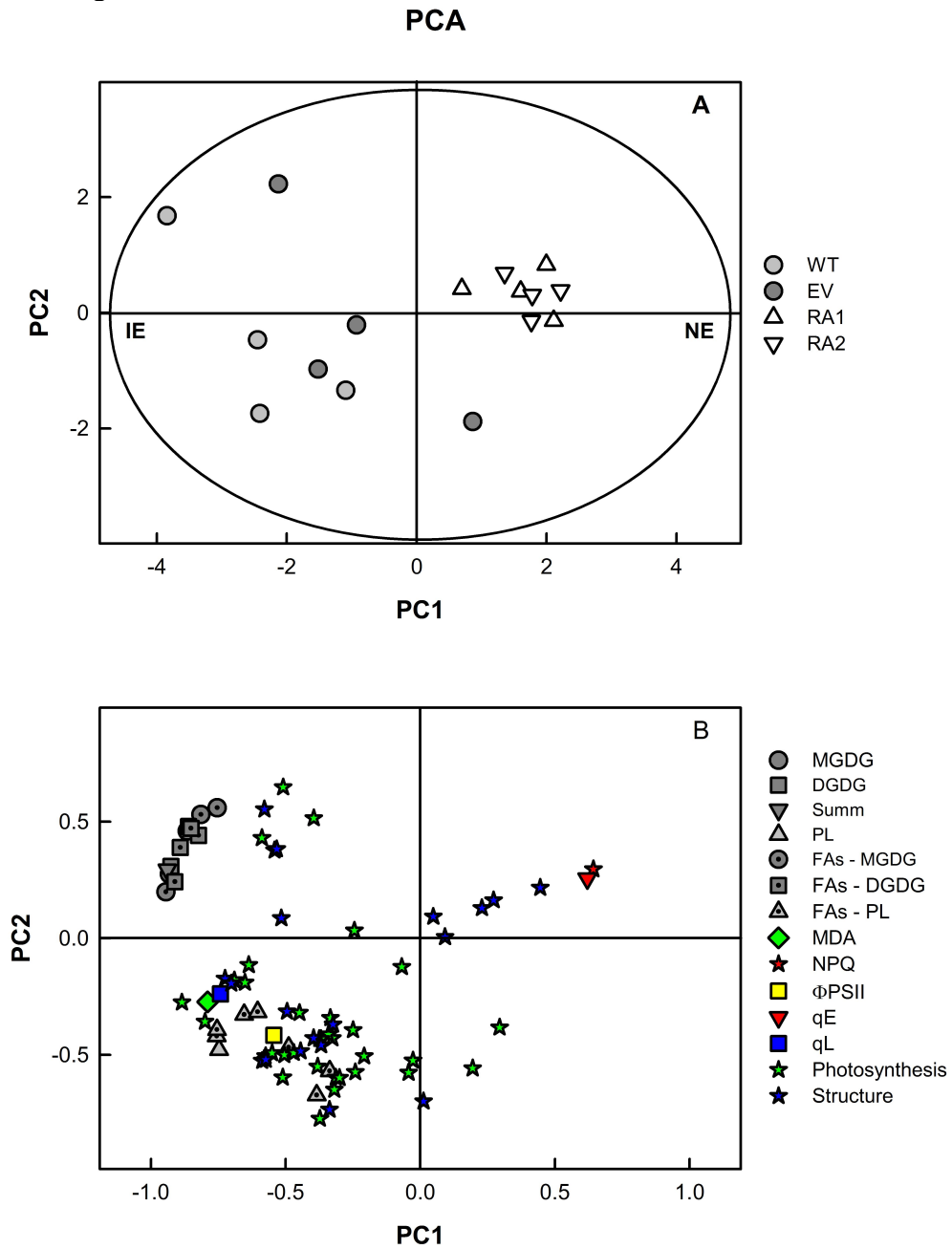


Fig. S2. Score and loading plots of PCA all parameters analyzed (lipid and fatty acid composition, MDA, NPQ, Φ_{PSII} , qE, qL, proteins related to photosynthesis and proteins with structural activity). (A) IE (WT/EV), grey circles; NE (RA1/RA2), white triangles. (B) Each parameter is indicated with different symbol. Dark grey circles, MGDG; dark gray square, DGDG; gray triangle, PL; dark gray circles with a dot, MGDG – fatty acids; dark gray square with a dot – DGDG – fatty acids; gray triangle with a dot, PL – fatty acids; green diamond, MDA; red star, NPQ; red triangle-down, qE; blue square, qL; blue star, proteins with structural activity; green star, proteins related to photosynthesis. Data with VIP > 1 (all data except proteins) and VIP > 0.5 (proteins) are presented.